Doctoral School in Neuroscience

Curriculum: Neuroscience and Neurotechnologies

Coordinator: Flavio Mariano Nobili

Cicle XXXV

Impaired excitatory and inhibitory synaptic plasticity in the NLGN3^{R451C} mouse model of autism spectrum disorder

Author: Martina Bruno

Supervisors: Andrea Barberis

Enrica Petrini

Università di Genova

ISTITUTO ITALIANO DI TECNOLOGIA

TABLE OF CONTENTS

ABSTRACT

Autistic spectrum disorder (ASD) has been associated to genetic alterations of proteins involved in synaptic function such as the point mutation R451C in neuroligin 3 (NLGN3), a postsynaptic adhesion molecule which binds its presynaptic partner neurexin at both excitatory and inhibitory synapses. In the present study, by exploiting the transgenic NLGN3-R451C knock-in (KI) mice as an ASD animal model, we aimed at investigating the role of this mutation in the coordination of both excitatory and inhibitory synaptic plasticity. We found that, in basal conditions, the $NLGN3^{R451C}$ protein was less expressed at the neuronal surface and showed increased lateral diffusion at GABAergic synapses with respect to WT condition. However, in spite of these differences, we observed comparable basal synaptic excitatory and inhibitory transmission in both KI and WT mice. Next, we tested WT and KI neurons for the expression of synaptic plasticity. In WT animals, we found that, in response to a chemical protocol for the induction of plasticity (NMDA treatment), excitatory synaptic currents were depressed (LTD) whereas the inhibitory ones were potentiated (iLTP). Interestingly, such opposed synaptic plasticity was abolished in KI neurons. These effects were paralleled by increased immunoreactivity for GABAAR and the scaffold protein gephyrin at synapses. Along the same line, NMDA treatment induced the decrease of the GluA1 and GluA2 subunits of AMPA receptors in WT mice, whereas the same protocol left AMPARs unchanged in KI mice. In contrast, no significant changes in molecular composition were observed in KI mice at both excitatory and inhibitory synapses. In addition, the quantification of NLGN3 clusters fluorescence intensity revealed that, after the NMDA treatment, surface NLGN3 decreased in WT neurons while it was unaffected in KI neurons. Moreover, in KI conditions, we found changes in the expression of the GluN2B subunit of NMDA receptor that may determine the altered coordination of excitatory and inhibitory plasticity through the perturbation of intracellular spatio-temporal calcium dynamics. Collectively, our results reveal that the perturbed synaptic molecular composition of both glutamatergic and GABAergic synapses induced by the NLGN3-R451C mutation disrupts the coordination of excitatory and inhibitory synaptic plasticity thus potentially contributing to the pathophysiology of ASD.

INTRODUCTION

1. Autism spectrum disorder risk genes

Autism spectrum disorder (ASD) refers to a broad range of conditions characterized by challenges with verbal and non-verbal communication, social interaction, and repetitive or restricted behaviors. Autism is a lifelong disability, which can be diagnosed at any age, but it is commonly considered as a "developmental disorder" because symptoms generally start to appear early in childhood (Rutter, 1978). The World Health Organization estimates that, nowadays, autism has a prevalence of ~1% within children (Zeidan et al., 2022) and affects 65 million people worldwide. Several developmental, environmental and genetic risk factors for ASD have been identified to cause this disorder, suggesting that the etiology of ASD is multifactorial (Happè et al. 2006; Bolte et al., 2018; Hallmayer et al., 2011). Over the last decade, ASD genetics has gained increasing attention since nearly 1% of non syndromic forms of ASD have been ascribed to a genetic origin. Indeed, genetic testing approaches such as chromosomal microarray and next-generation sequencing have recently accelerated the identification of inherited and de-novo genetic alterations representing causative – or susceptibility – factors for both mild and severe autism. To date, more than 100 genes have been identified to show a strong link with ASD (Iossifov et al., 2012; Sanders et al., 2012; Neale et al., 2012; O'Roak et al., 2012). The large heterogeneity of the genetic causes of ASD can account for its phenotypic heterogeneity and pave the way for new diagnostic procedures and future personalized therapies. Moreover, the complexity and the diversity of clinical presentations of ASD are possibly due to gene-environment interactions, which are thought to be mediated by epigenetic modifications in response to exposure to environmental modifiers that influence gene expression (Bacchelli et al., 2006; Yuen et al., 2015). Nevertheless, the influence of genetic alterations on the development of ASD is supported by many factors:

- the high heritability - approximately 80% (Sandin et al., 2017);
- the sex distribution - ASD is four times more common in males than females (Baio et al., 2018; Loomes et al., 2017);
- the larger prevalence in siblings - up to 20% (Ozonoff et al., 2011; Constantino et al., 2010; Palmer et al., 2017);

- the high concordance in monozygotic twins (around 59%) and increased risk of ASD with increased relatedness - 3% for cousins, 7% for paternal half-siblings, 9% for maternal half-siblings, 13% for full siblings and dizygotic twins (Sandin et al., 2014).

ASD can be caused by a single genetic defect (monogenic ASD) or driven by multiple genetic alterations (polygenic ASD). Monogenic mutations can account for either syndromic autism, such as Fragile X syndrome, Rett syndrome, tuberous sclerosis (TSC) and Angelman syndrome, or non-syndromic autism, also called idiopathic autism, which represents 90% to 95% of cases (Gillberg 1996; Boddaert et al., 2006). Numerous ASD candidate genes are involved in synapse formation and function, leading to the concept of ASD as a 'synaptopathy' (Kleijer et al., 2014; Zoghbi et al., 2012). Among them, a prominent causal role is played by the *Nrxn*, *Nlgn*, *Shank*, *TSC1/2*, *FMR1* and *MECP2* genes (Baig et al., 2017). These genes encode cell adhesion molecules or scaffolding proteins, which affect various aspects of synapses, including synapse formation and elimination, synaptic transmission and plasticity (Guang et al., 2018). However, it must be underlined, that synaptic protein genes account only for the minority of ASD cases. Indeed, the molecular pathways implicated in ASD also include transcriptional regulation and chromatin-remodeling (De Rubeis et al., 2014), protein translation and modification, neuroimmunological modulation and mitochondrial function (De Rubeis and Buxbaum, 2015; Loke et al., 2015; Mahfouz et al., 2015; Subramanian et al., 2015; de la Torre-Ubieta et al., 2016; Wen et al., 2016). Although, the pathogenesis of ASD can only be partially attributed to synaptic dysfunction, mutations in synaptic proteins can "efficiently" disrupt the synaptic network and brain function, thus making synapses a privileged site for the study of ASD.

One of the most recurrently affected pathway is represented by the trans-synaptic signaling involving NRXNs/NLGNs in which NLGNs play an important role in synapse identity and in synaptic maturation and homeostasis (Zhang et al., 2015). Indeed, NLGNs are involved in the formation of either glutamatergic or GABAergic synapses, therefore contributing to the maintenance of the appropriate excitatory/inhibitory ratio (E/I) in specific neural connections (Craig and Kang, 2007; Levinson and El-Husseini, 2005).

Several de novo and inherited mutations in human neuroligin genes have been found to be associated with ASD (Nakanishi et al., 2017; Jamain et al., 2003) and in particular, among neuroligins isoforms, NLGN3 appears to be a recurrent target for these mutations. The first link between ASD and NLGN3 was identified in a Swedish family with two affected brothers, one with ASD and the other with Asperger's syndrome (Jamain et al.2003). Both probands

contain a missense mutation in *Nlgn3* (NLGN3 R451C), which encodes an arginine instead of a cysteine at amino acid 451 within the extracellular domain (ECD) of NLGN3. Starting from this study case, an increasing body of evidence reinforces the idea that NLGN3, and adhesion molecules in general, play an important role in autism's pathophysiology. Interestingly, NLGN3 can be found at both excitatory and inhibitory synapses suggesting that it is potentially a molecular substrate for the functional interplay between excitation and inhibition.

2. Excitatory/Inhibitory balance and homeostasis in autism spectrum disorder

Twenty years ago, John Rubenstein and Michael Merzenich proposed that autism and related disorders might reflect an increase in the ratio between excitation and inhibition causing hyper-excitability of cortical circuits (Rubenstein and Merzenich, 2003). Since then, other studies have suggested the disruption of the balance between excitation and inhibition as one of the proposed etiological mechanisms of ASD (Oliveira et al., 2018; Bozzi et al., 2018). This theory provided a potential explanation for the frequent observation of reduced GABAergic signaling in the autistics brains (Cellot and Cherubini, 2014), as well as their propensity to develop epilepsy (Bolton et al., 2011). However, other studies have found evidence for decreased excitation in ASD as well, suggesting that both excitatory and inhibitory properties are affected in ASD patients (Etherton et al., 2009; Smith et al., 2017). In this concern, studies on transgenic mouse models of ASD provide support for this E/I imbalance hypothesis reporting reduced inhibition (Chao et al., 2010; Gibson et al., 2008; Han et al., 2012; Liang et al., 2015; Mao et al., 2015), decreased excitation (Dani et al., 2005, Delattre et al., 2013, Unichenko et al., 2018, Wood and Shepherd, 2010) or also increased inhibition (Harrington et al., 2016, Tabuchi et al., 2007). This framework is even more complicated if we consider the differences across studies in different brain area, cell type and ASD genotype, resulting in the lack of identification of common synaptic and local circuit defects in ASD. Thus it is becoming increasingly evident that the idea of "E/I balance" determining whether brain circuits are normal or "autistic" is oversimplified and that the "E/I balance hypothesis", that for decade represented a framework for understanding the pathophysiology of ASD, needs to be revised. In addition, the concept of E/I "balance" or "ratio" is still ill-defined. For instance, in the time domain, at short time scales (millisecond range), the amount of synaptic excitation and inhibition received by a given neuron is not necessarily "balanced". Such temporal mismatch of excitatory and inhibitory input activation allows neurons to express spiking pattern with complex time structures. At

longer time scales, in contrast, the integrated activation of excitatory and inhibitory inputs tends to balance in order to prevent runaway activity. In the space domain, it has been shown that the numbers of excitatory and inhibitory synapses on individual cortical pyramidal neurons are highly regulated by a process that generates a relative invariant ratio of E/I synapses across dendritic regions (Iascone et al., 2018). Nevertheless, while the total number of excitatory and inhibitory synapses determines a "balanced" activity in a certain dendritic region, excitatory and inhibitory synapses may still be "unbalanced" in specific dendritic sub-regions where, for instance, an uneven synaptic distribution may locally cluster excitatory or inhibitory synapses. Such "patchy" configuration may influence the generation of dendritic spikes that can be promoted by the activation of few contiguous clustered excitatory synapses on dendritic branches (Polsky et al., 2004). The concept of local synapse clustering is particularly relevant since in the dendrites of neocortical or hippocampal pyramidal neurons, excitatory and inhibitory inputs are highly compartmentalized in neuronal sub-regions. For instance, pyramidal neurons (PNs) of the CA1 hippocampal area receive inputs from the entorhinal cortex and thalamus in distal dendrites while Schaffer collaterals from CA3 and fibers from amygdala contacts the proximal and the basal dendrites. Similar compartmentalization is also observed at inhibitory inputs since CA1 PNs is contacted by different subtypes of inhibitory interneurons in specific regions along the axo-dendritic axis. Fast-spiking interneurons expressing parvalbumin (PV^+-INs) (basket cells) target the perisomatic region of PNs and exert an important role in setting the network clock and by controlling the action potential generation. Cholecystokinin positive interneurons (CCK^+-INs), that also contact PNs in the perisomatic region, show regular firing pattern and provide a slower but highly modulated control of postsynaptic activity. Oriens-Lacunosum-Moleculare interneurons (OLM) neurons form contacts on both dendritic shafts and spines of PNs precisely controlling dendritic integration. They are somatostatin (SOM^+) positive neurons that restrict the temporal and spatial spread electrical signals in CA1-PNs dendrites. Similarly, bistratified interneurons (BiS-INs) target the CA1-PNs more proximal dendrites and basal dendrites. In this scenario, it is clear that excitatory and inhibitory inputs in PNs micro-domains can form dendritic "nodes" in which a specific local E/I ratio can be established. Therefore, E/I may vary from one cellular component to another and despite a stable global level of balanced excitation and inhibition, neurons may show local imbalance. In this view, it could be possible that, in ASD, specific dendritic micro-domains are selectively perturbed, thus leading to subtle alterations of the functional network. Overall, by considering the aforementioned concepts, the excitatory-to-inhibitory ratio could

still be an important determinant for the ASD pathogenesis if considered both dynamically and locally.

To further complicate the picture, it is not obvious to understand whether the altered E/I balance observed in ASD is either cause or effect of ASD. In relation to this, a recent study showed that while the synaptic E/I ratio was increased in four different mouse models of autism, the neuronal spiking activity in each of these four models matched that of wild type (Antoine et al., 2019). The authors propose that homeostatic synaptic plasticity induced by the autism-related mutations determines an imbalance of the excitation-to-inhibition ratio aimed to overall restore the spiking activity and network activity. In these conditions, the autistic phenotype could be generated by subtle differences in spiking pattern activity between ASD models and wild types. Alternatively, the fact that the "dynamic range" of synaptic plasticity is employed for such homeostatic compensation makes synapses unable to undergo correct plasticity event in response to external stimulation. Previous studies addressing homeostatic plasticity could provide a possible framework for a possible compensatory effect observed in ASD models. For instance, it has been shown that both excitatory and inhibitory synapses exhibit robust homeostatic plasticity that adjusts E-I ratio to stabilize cortical firing rate (Gainey and Feldman, 2017; Turrigiano 2011) or restore a predetermined set point following perturbations (Davis, 2006; Marder and Goaillard, 2006; Pozo and Goda, 2010; Turrigiano, 2011; Turrigiano and Nelson, 2004). These mechanisms of plasticity typically involve changes in the strength and the number of excitatory and inhibitory synapses but can also be achieved by changes in the intrinsic neuronal excitability.

3. Synaptic transmission and plasticity at excitatory and inhibitory synapses

One of the most important and fascinating properties of the brain is the ability to undergo plasticity. Synaptic plasticity is the fundamental mechanism by which the neural activity generated by an experience modifies brain function. Activity-dependent modification of the strength or efficacy of synaptic transmission is believed to play a key role in learning and memory. Given the importance of synaptic plasticity for any organism to successfully interact with its environment, it is not surprising that several types of plasticity have been described across neuronal types, brain regions and animals models in order to elucidate this phenomenon at several levels from the molecular to circuit and behavior. Synaptic transmission can be either enhanced or depressed by activity, and these changes can last from milliseconds to hours, days,

and lifelong. For decades, studies of synaptic plasticity have largely focused on excitatory glutamatergic connections, while the GABAergic counterpart has been only marginally investigated. However, a growing body of evidence demonstrates the capacity of inhibitory synapses to express several forms of plasticity both at pre and postsynaptic levels. Moreover, it has been clearly shown that several molecular players involved in the excitatory plasticity are also acting at inhibitory synapses (Chiu et al., 2018; Flores et al., 2015; Marsden et al., 2007; Petrini et al., 2014) highlighting possible functional interactions between glutamatergic and GABAergic plasticity both in physiological and pathological states.

3.1 Synaptic plasticity at glutamatergic synapses

The primary subtypes of glutamate receptors expressed at glutamatergic synapses are the α-amino-3-hydroxy-5-methylisoxazole-4-propionic acid (AMPA) and N-methyl-d-aspartate (NMDA) subtypes. The AMPA-type glutamate receptors are important in determining post-synaptic cell excitability, because they conduct most of the current flow at resting membrane potentials (Sommer et al., 1992) while the NMDA-type due to the voltage-dependent magnesium blockade, is able to conduct current only at depolarized membrane potentials (Morris et al., 1989). AMPA receptor is an ionotropic transmembrane receptor composed of four types of subunits named GluA1, GluA2, GluA3, GluA4 which combine to form tetramers. Most AMPARs are heterotetrameric, consisting of symmetric 'dimer of dimers' of GluA2 and either GluA1, GluA3 or GluA4 (Greger et al., 2007). NMDA receptors are also heterotetramers and they are composed of two GluN1 and typically two GluN2 subunits (Salussolia et al., 2011). Glutamate receptors are anchored at excitatory synapses through a network of scaffolding proteins located at the post-synaptic dendritic spine in a region called post-synaptic density (PSD). PSD-95 and Homer proteins are the most abundant scaffolding proteins that are present at the post-synaptic terminal of glutamatergic synapses. The NMDA receptor is crucial for synapstic plasticity and it has been defined ‘coincidence detector’ because both glutamate and depolarization are required to relieve NMDARs of magnesium block so that they allow calcium influx, which triggers long-term potentiation (LTP) of synaptic connections (Sjöström & Nelson, 2002). Briefly, in response to afferent activity induced depolarization of the post-synapse coincident with presynaptic transmitter release, calcium influx through the NMDA receptor triggers the active insertion or removal of AMPA-type glutamate receptors (Genoux et al., 2007). The increase of synaptic strength is called long-term potentiation (LTP), whereas

the decrease of synaptic strength is termed long-term depression (LTD). In general, changes of AMPA receptors number determine the expression of synaptic plasticity, whereas the calcium entry mediated by NMDA receptor activity is largely responsible to modulate the intracellular machinery controlling AMPA receptor insertion/removal. Glutamatergic plasticity was first described in 1973 by Tim Bliss and Terje Lømo (Bliss and Lømo, 1973); since then, many studies addressed the different forms of glutamatergic plasticity. The mechanisms of plasticity were extensively studied in the mammalian hippocampus at synapses made by the Schaffer collaterals (axons of CA3 pyramidal cells) onto the CA1 pyramidal neurons. Theta burst stimulation, repeating pattern of short high-frequency (100Hz) burst at the theta rhythm (5 to 7 Hz), induced LTP, while low frequency stimulation (1Hz, 900 pulses) were responsible for LTD (Kirkwood et al., 1993). This form of plasticity is based on the coincidence of pre- and postsynaptic activity (Hebbian plasticity) that cause a Ca^{2+} influx through NMDA receptors, triggering a CaMKII dependent cascade of activation that, in turn, lead to changes in the number of synaptic AMPA receptors. Interestingly, Ca^{2+} may lead to either LTP or LTD depending on its intracellular spatiotemporal profile, which, in turn, is determined, by the length, the pattern and the duration of the neuronal stimulation. In case of LTP, Ca^{2+} entry into the spine activates Ca^{2+}/ calmodulin- dependent protein kinase 2 (CaMKII) and causes its dissociation from actin and translocation into the PSD (Zhang et al., 2008). In contrast, following the low frequency stimulation, the activation of the calcineurin induces a dephosphorylation of the AMPA receptors at the synapse, promoting an endocytosis and leading to an LTD (Lee and Kirkwood, 2011). While the aforementioned forms of synaptic plasticity are expressed postsynaptically, other forms of plasticity are expressed at presynaptic level. A well-known example was identified in the hippocampus, at synapses formed by dentate gyrus (DG) granule cells and CA3 neurons (mossy fibers). In these synapses, high frequency stimulations trigger an increase in the probability of glutamate release (Mellor and Nicoll, 2001; Zalutsky and Nicoll, 1990). In particular, the increase of calcium concentration in the presynaptic terminal mediated by R-type voltage gated calcium channels (VGCC) leads to the activation of PKA which in turn phosphorylates the active zone proteins Rab3A and Rim1a increasing the release probability of the neurotransmitter (Castillo et al., 1997, 2002; Nicoll and Schmitz, 2005) ending with LTP. The same synapses, under different conditions, could also show presynaptic LTD mediated by the metabotropic glutamate receptors mGluR2 located on the presynaptic neuron (Kobayashi et al., 1996; Kobayashi et al., 1999; Tzounopoulos et al., 1998). The stimulation of the G protein decreases the activity of the PKA, leading to LTD, resulting in a reduction in vesicles release (Castillo, 2012).

3.2 Synaptic plasticity at GABAergic synapses

Fast synaptic inhibition relies on the enrichment of type A GABA receptors (GABAARs) at postsynaptic sites. GABAARs are ligand-gated ionotropic receptor channels and consists of five subunits arranged around a central pore, which is permeable to Cl^- and bicarbonate ions (Unwin, 1995). GABAARs have been found to belong to the superfamily of Cys-loop ligand gated receptors and assembled in heteropentamers from the combination of 19 subunits: α(1–6), β(1–3), γ(1–3), δ, ε, θ, π and ρ(1–3) (Barnard et al., 1998; Sieghart, 2006). Although thousands of different receptor combinations could be potentially assembled, GABAARs preferred assemblies in the brain are mostly composed by two copies of a single α, two copies of a single β, and one copy of γ, δ, or ε (Sieghart and Sperk, 2002; Whiting, 2003). The inhibitory postsynaptic density (iPSD), includes a variety of molecular components determining the localization, stability and regulation of GABAA receptors. Gephyrin is one of the major postsynaptic scaffolding protein and has been first proposed to self-oligomerize and to create a synaptic lattice able to trap and accumulate GABAA receptors at synaptic sites (Kneussel and Betz, 2000b; Moss and Smart, 2001). However, several studies have shown that the molecular organization of postsynaptic element at inhibitory synapses is rather due to the dynamic interaction of different molecules including gephyrin, collibystin, neuroligin 2 and the GABAA receptors (Kim et al., 2006; Sola et al., 2004).

The synaptic inhibition mediated by GABAARs is critical to shape the postsynaptic spiking output, so it is unsurprising that these connections also exhibit various forms of long-term plasticity that play critical roles in modulating neuronal activity. Among the best characterized forms of inhibitory plasticity are those expressed at the presynaptic level (Hartman et al., 2006; Peng et al., 2010). Presynaptic inhibitory plasticity mainly relies on the modification of presynaptic GABA release through the action of retrograde messengers produced in the postsynaptic neuron in an activity-dependent manner and, after release, travel backward to the presynaptic terminal to modulate the neurotransmitter release (Regehr et al., 2009). Such retrograde messengers include endocannabinoids (eCBs), nitric oxide (NO) and peptides as neurotrophic factors such as BDNF. For example, eCBs are synthetized in the postsynaptic terminal and then mobilized to the presynaptic terminal, where they bind and activate G-protein-coupled type I cannabinoid receptors (CB1) to suppress the neurotransmitter release either in short-term or long-term manner (Chevaleyre et al., 2007; Diana and Marty, 2004; Freund et al., 2003; Heifets et al., 2008; Kano et al., 2009). In the neocortex and hippocampus,

the principal eCBs messengers are the 2AG (2- arachidonoylglycerol) and the anandamide (Chevaleyre et al., 2006; Harkany et al., 2004; Heifets and Castillo, 2009). Retrograde eCBs signalling can lead to depolarization-induced suppression (DIS) of inhibition in the hippocampus (Ohno-Shosaku et al., 2001; Wilson and Nicoll, 2001), in which the depolarization of pyramidal neurons triggers Ca^{2+} entry through voltage-gated Ca^{2+} channels (VGCCs) and NMDA receptors leading to the synthesis of 2-AG. The consequent release and diffusion of eCBs activate the G-protein coupled with CB1 receptor located presynaptically which in turn reduces the calcium influx in the presynaptic terminal through the inhibition of VGCC, thus affecting the release of GABA from interneurons and promoting inhibitory depression (Chevaleyre et al., 2007; Kano et al., 2009). Depolarization induced-suppression of inhibition (DSI) is a short-term form of eCB-mediated plasticity but eCBs are also implicated in presynaptic forms of long-term depression (LTD) at both excitatory (Gerdeman et al., 2002; Robbe et al., 2002) and inhibitory (Chevaleyre and Castillo, 2003; Marsicano et al., 2002) synapses. For long-term plasticity, the predominant mechanism requires inhibition of adenylyl cyclase and downregulation of the cAMP/PKA pathway through the activation of the α subunit of G protein of CB1 receptors resulting in the persistent depression of inhibitory synaptic transmission (Chevaleyre et al., 2006; Heifets and Castillo, 2009). eCBs are also implicated in a form of heterosynaptic LTD. This mechanism requires that glutamate from neighboring excitatory synapses activate metabotropic glutamate receptors I (mGluR-I), present at the GABAergic presynaptic terminal, hyperpolarizing the GABAergic interneuron and preventing its firing during 2-AG synthesis (Heifets and Castillo, 2009). Concomitantly, the activation of CB1Rs by 2-AG results in a decrease of the PKA transduction cascade. At inhibitory synapses, decreased PKA activity, in conjunction with activation of the Ca^{2+}-sensitive phosphatase calcineurin (CaN), shifts the phosphorylation status of an unidentified presynaptic target causing a long-term decrease in GABA release (Castillo et al., 2011).

In addition to presynaptic expression, the flexibility of inhibitory synapses can also rely on postsynaptically expressed plasticity. In analogy with excitatory synapses, postsynaptic forms of synaptic plasticity mainly rely on the modification of the synaptic receptor number that, in turn, is regulated by receptor trafficking (endo- and exocytosis) and receptor lateral diffusion on the plasma membrane (Petrini et al., 2014). In this concern, it has been found that, for instance, activation of NMDA receptors determined the activation of CaMKII with consequent accumulation and stabilization of GABAA receptors at synapses and increase of inhibitory synaptic currents (iLTP) (Nusser et al., 1998; Marsden et al., 2007; Kurotani et al., 2008; Petrini

et al., 2014). In contrast, inhibitory long-term depression (iLTD), has been found to depend on the reduced availability of GABAARs at synapses through GABAA receptor internalization or GABAA receptor dispersal from the synapse which depended on the activation of the phosphatase calcineurin (Kurotani et al., 2008; Bannai et al., 2009; Muir et al., 2010; Pertrini et al., 20014; Marsden et al., 2007).

High-frequency action potentials in cortical layer 5 PNs can drive potentiation of perisomatic inhibition via calcium entry through R-type voltage-gated calcium channels (Kurotani et al., 2008). Remarkably, the same stimulation at hyperpolarized membrane triggers the calcium influx through the L-type VGCC resulting instead in a weakening of the synaptic strength. Interestingly, both the effects are prevented by adding botulinum toxin that interferes with the constitutive GABAA receptor recycling and trafficking (Chiu et al., 2019; Kurotani et al., 2008). Similarly, in the cerebellum another form of postsynaptic iLTP, called rebound potentiation, involves the depolarization of the Purkinje cells mediated by excitatory inputs coming from climbing fibers (Kano et al., 1992).

Finally, many works have highlighted that the different classes of interneurons not only differ for features such as morphology, activity, synapses composition and location, but also differ in the induction of plasticity. It has been showed that in the cerebellum the depolarization of a Purkinje cell potentiated the strength of somato-dendritic basket cell synapses without affecting distal dendritic stellate cell synapses (He et al., 2015). This form of plasticity is allowed by the β2-subunit-containing GABAA receptors, which are predominantly expressed in basket cells. Moreover, in the cortex the stimulation of NMDA receptors with a chemical protocol, was able to potentiate the distal inhibitory synapses formed by SST^+ interneurons without affecting the transmission of perisomatic synapses of PV^+ interneurons (Chiu et al., 2018). A different work focused on the hippocampus showed the same interneuron specific plasticity: during a physiological activity pattern, the currents mediated by the activation of SST^+ interneuron were potentiated while transmission mediated by PV^+ interneurons was depressed (Udakis et al., 2020). Therefore, under specific condition, the synapses located in different part of the neurons can be differently influenced, for this reason the localization of a synapse on the dendritic tree can be crucial for ultimately shaping neuronal output.

3.3 Interplay between GABAergic and glutamatergic plasticity

As mentioned above, neuronal stimulation can regulate GABAergic transmission, leading to either long-term depression or potentiation of GABAergic synapses. Several studies have induced iLTP by means of a chemical protocol based on the activation of NMDA receptors (by NMDA) and the consequent activation of the CaMKII pathway (Marsden et al., 2007; Petrini et al., 2014; Wiera et al., 2021). These effect have been demonstrated to occur through different mechanism involving, for instance, the CaMKII phosphorylation of S383 on β3 GABAAR promoting the GABAAR immobilization and accumulation at inhibitory synapses (Petrini et al., 2014) and the gephyrin phosphorylation at S305 thus positively modulating gephyrin aggregation in CA1 PNs (Flores et al., 2015). Overall, this NMDA effects imply that glutamatergic activity is able to modify the strength of GABAergic synapses through a heterosynaptic interaction. Interestingly, the NMDA-based protocol used for GABAergic iLTP, in parallel, induces long term depression at excitatory synapses, (Marsden et al., 2007; Petrini et al., 2014). Since the NMDA protocol elicits mild intracellular Ca^{2+} elevation, it is tempting to hypothesize that glutamatergic or GABAergic plasticity obey to opposite calcium rules. This paradigm would be further validated by the observation that plasticity protocols eliciting massive calcium entry induce potentiation of glutamatergic and depression of inhibitory synapses through a calcineurin dependent mechanism that determines the dispersion of GABAA receptors and gephyrin from the synapse (Muir et al., 2010; Bannai et al., 2009; Niwa et al., 2012). A possible mechanism for such differential plasticity effect has been provided by the Marsden group who proposed that the mild NMDA receptor stimulation would induce the translocation of the activated CAMKII from excitatory to inhibitory synapses in dendrites (Marsden et al., 2010).

These findings also demonstrate that plasticity of glutamatergic and GABAergic synapses share similar regulatory pathways and may be locally coordinated. In this scenario, calcium concentration can regulate the bidirectional plasticity of both excitatory and inhibitory synapses determining the fine control of the excitation-to-inhibition balance (E/I).

4. Cell adhesion molecules

Synapses are highly specialized sites of asymmetric cell–cell adhesion, which is an important structural and functional aspect of synapses and it is carried out by cell adhesion molecules

(CAMs) (Akins and Biederer 2006; Piechotta et al. 2006). The regular width of the synaptic cleft shows that adhesive interactions act as "molecular rulers" to define its span (Palade and Palay 1954; Gray 1959). During synaptogenesis, the spatially and temporally coordinated assembly of pre- and postsynaptic membranes, axonal growth cones and their dendritic targets frequently extend filopodia to form initial contacts (Cooper and Smith 1992). The precise overlap of pre- and postsynaptic specializations assemble at these contacts until the intercellular distance widens from an initial 13 nm interstitial space to the final 20 nm "cleft" (Rees et al. 1976). It should be noted that CAMs not only represent the bridge between the pre and the post synaptic element but above all they play a key role in intercellular trans-synaptic signaling. Mature synapses are subjected to activity dependent structural and functional plasticity mechanisms that remodel them and that may be regulated by synaptic cell adhesion molecules (Toni et al. 1999; Knott et al. 2002). CAMs are actively involved in synapse formation and elimination that are essential process to support learning and memory throughout the lifetime of an organism. Synaptic cell adhesion molecules comprise a big number of proteins that are specialized for distinct functions in the recognition, molecular assembly, and/or specification of chemical synapses. There are different groups of CAMs: the integrin family, the immunoglobulin superfamily, the selectins, the cadherins, the neurexins (NRXNs) and the neuroligins (NLGNs) families in addition to a number of other glycoproteins. NRXNs and NLGNs are probably the best characterized synaptic cell adhesion molecules and they are expressed at both excitatory and inhibitory synapses (**Figure I**). They are trans-synaptic binding partners that exhibit synaptogenic activity in cell culture assays. In particular, using co-cultures between primary neurons and non-neuronal cells transfected with neurexins or neuroligins uncovered the ability of these molecules in stimulating the de novo formation of functional synapses by clustering presynaptic or postsynaptic proteins (Graf et al., 2004; Scheiffele et al., 2000). Recent studies have identified mutations in the genes encoding NRXNs and NLGNs as a cause for ASDs, Tourette syndrome, mental retardation, and schizophrenia, sometimes in patients with the same mutation in the same family (Feng et al., 2006; Macarov et al., 2007). The studies that have been carried out so far identify NRXNs and NLGNs as transsynaptic cell-adhesion molecules that mediate essential signalling between pre- and postsynaptic specializations, playing a central role in the brain's ability to process information that is a key target in the pathogenesis of cognitive diseases (Südhof, 2008).

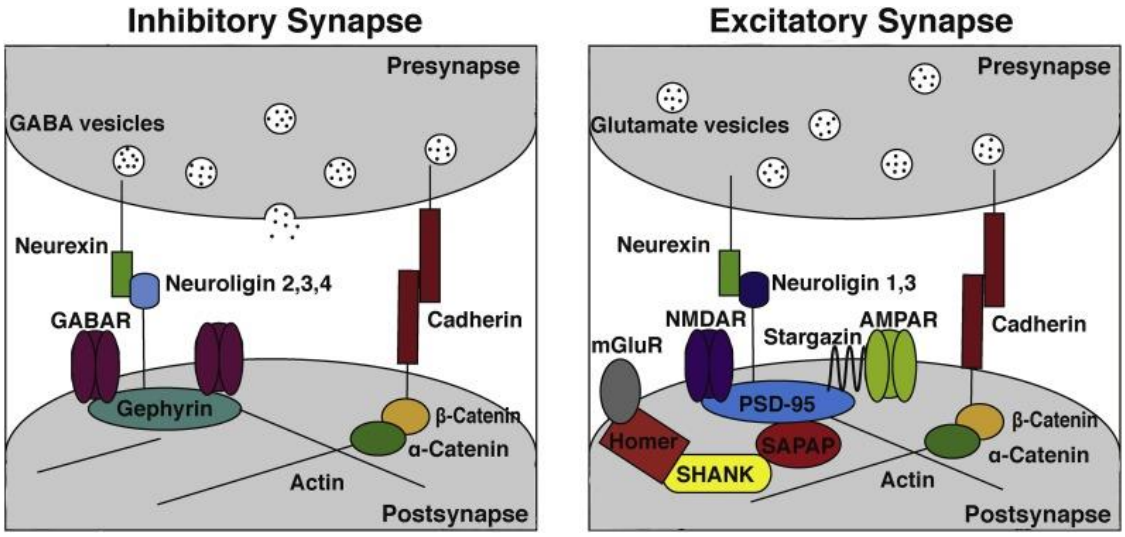

Figure I*. The differential organization of major synaptic structural proteins in inhibitory (left) and excitatory (right) synapses. Presynaptic neurexins interact with postsynaptic neuroligins, which have synapse specific isoforms and interactions (Howell and Smith, 2019).*

4.1 Neurexins and Neuroligins: structure and function

Neurexins

Neurexins (NRXNs) were originally discovered as receptors for α-latrotoxin, a vertebrate-specific toxin of Black widow spider venom. α-latrotoxin is a large protein that binds to presynaptic receptors and induces massive neurotransmitter release (Ushkaryov et al. 1992, 1994). NRXNs are type 1-membrane proteins that come in two isoforms: larger α-NRXNs, and shorter β-NRXNs. α- and β-NRXN contain different N-terminal extracellular sequences, but identical C-terminal transmembrane regions and cytoplasmic tails (Südhof, 2008). Extracellularly, α-NRXNs have six LNS-domains [laminin/neurexin/sex hormone-binding globulin-domain] with three intercalated EGF-like domains, whereas β-NRXNs have a single LNS domain (Ushkaryov et al. 1992, 1994). Neurexins are extensively alternatively spliced at five conserved sites in their extracellular region, creating potentially thousands of isoforms (Ullrich et al. 1995; Tabuchi and Sudhof 2002). The short cytoplasmic tails of NRXNs contain PDZ-domain binding sequences that bind to key proteins in the presynaptic machinery (Hata et al., 1996; Biederer and Südhof, 2001). The importance of NRXNs is highlighted by the fact that neurexins are evolutionarily conserved and pan-neuronally expressed (Tabuchi and Sudhof 2002; Haklai-Topper et al. 2011). Vertebrates contain three neurexin genes (*neurexin-1* to *-3*) each of which directs transcription of α- and β-NRXNs from independent promoters (Ulrich et al., 1995).

Neuroligins

Neuroligins (NLGNs) are postsynaptic type I membrane proteins that were identified as neurexin ligands (Ichtchenko et al., 1995 and 1996). NLGNs are composed of an extracellular acetylcholinesterase homology domain without esterase activity, a highly conserved single transmembrane domain and a cytoplasmic tail with PDZ domain binding motif (Ichtchenko et al., 1996). The extracellular sequence of neuroligins forms a constitutive dimer, whereas their cytoplasmic tails contain the PDZ-domain binding sequence that recruits PSD-95 and other PDZ-domain proteins (Irie et al., 1997), and tyrosine-based motif that binds to gephyrin (Poulopoulos et al., 2009). Neuroligins are expressed from four genes in vertebrates (*Nlgn1, Nlgn2, Nlgn3, Nlgn4*) with the NLGN3 and NLGN4 gene in humans localized to the X-chromosome. Humans and primates in general, contain non-recombining copies of neuroligin-4 on the X- and Y-chromosomes, with the Y-chromosomal copy often referred to as neuroligin-5 (*Nlgn5*) or neuroligin-4Y (*Nlgn4Y*). In contrast to neurexins, neuroligins are specifically localized to particular synapses. NLGN1 is only present at excitatory synapses (Song et al. 1999), NLGN2 and NLGN4 at inhibitory synapses (Varoqueaux et al. 2004; Hoon et al. 2011), whereas NLGN3 is present at both excitatory and inhibitory synapses (Budreck and Scheiffele 2007). Recent data also show that NLGN4 in the retina is preferentially localized to glycinergic postsynapses (Hoon et al,. 2011).

Neuroligins and Neurexins interaction and function

NLGNs bind to both α- and β-NRXNs with nanomolar affinities, the binding involves the sixth LNS domain of α-NRXNs which corresponds to the only LNS-domain of β-NRXNs (Comoletti et al., 2006). Moreover, different neurexin and neuroligin isoforms show distinct binding affinities. However, binding of neurexins and neuroligins is tightly regulated by alternative splicing, especially at the splice site 4 in the shared LNS-domain of α- and β-neurexins (Ichtchenko et al. 1995; Boucard et al. 2005). Interestingly, contact of dissociated neurons with neuroligin-expressing non-neuronal cells results in the recruitment of presynaptic markers (Scheiffele et al. 2000), whereas contact of neurons with neurexin-expressing non-neuronal cells produces recruitment of postsynaptic markers (Graf et al., 2004; Nam and Chen 2005). As mentioned before, NLGNs expression in a non-neuronal cell can induce co-cultured neurons to form presynaptic specializations onto the non-neuronal cell (Scheiffele et al., 2000) while

NRXNs, when expressed in a non-neuronal cell, can induce formation of postsynaptic specializations in co-cultured neurons (Graf et al., 2004). Moreover, overexpression of neuroligins in neurons leads to dramatic increases in neuronal synapse density (Chih et al., 2005; Boucard et al. 2005), whereas deletion of neuroligins does not decrease synapse density (Varoqueaux et al., 2006). Another group of studies of knockout mice has revealed vital functions for α-neurexins and neuroligins in the synapse organization. The combined knockout of all three α-neurexins is lethal at birth (Missler et al., 2003; Zhang et al., 2005a) probably due to a strong impairment in neurotransmitter release. Even single α-neurexin knockout mice show a survival phenotype and, in particular, neurexin-1α single knockout mice display decreased excitatory transmission in the hippocampus and behavioral deficits (Etherton et al., 2009). Triple knockout of NLGN1, NLGN2, and NLGN3 also results in perinatal lethality caused by an impairment of synaptic transmission (Varoqueaux et al., 2006). Interestingly, consistent with its localization, the single knockout of NLGN1 selectively impairs the strength of excitatory synapses and decreases the ratio of NMDA- to AMPA-receptor mediated responses, whereas single knock out of NLGN2 selectively depresses inhibitory synaptic transmission (Chubykin et al., 2007; Poulopoulos et al., 2009). NLGN3 KO and NLGN4 KO mice exhibit selective deficits in social interactions and communications. Studies on ultrasonic vocalization showed, about 3-fold increase in latency of start calling and 48% reduction in total number of calls in KO male mice together with higher motor activity in both open field tests and elevated plus maze tests (Jamain et al., 2008; Radyushkin et al., 2009). These findings indicates that α-NRXNs and NLGNs, are essential for proper assembly of synapses into fully functional units. Indeed, alterations in synaptic genes encoding NRXNs and NLGNs and their interaction partners play determinant roles in the pathogenesis of ASD. Mutations in the genes encoding NRXN1, NLGN3 and NLGN4 have been associated with familial ASDs. Specifically, seven point mutations, two distinct translocation events, and four different large-scale deletions in the NRXN1 gene were detected in autistic patients (Feng et al., 2006; Marshall 2008). Concerning neuroligins, ten different mutations in the NLGN4 gene (2 frameshifts, 5 missense mutations, and 3 internal deletions) and five different larger deletions of X-chromosomal DNA that includes the NLGN4 locus were detected in autism patients (Marshall 2008; Chocholska et al., 2006; Lawson-Yuen et al., 2008). One of the best characterized ASD related mutation is R451C missense mutation in NLGN3 gene (Jamain et al., 2003) involved in a non-syndromic monogenic form of ASD.

4.2 Neuroligin 3

NLGN3 structure and interactions

NLGN3 is the only NLGNs isoform localized at both excitatory and inhibitory synapses. Several lines of evidence have suggested that the unique expression and function of NLGN3 protein underlie circuit-specific dysfunction characteristic of non-syndromic ASD caused by the disruption of NLGN3 gene (Uchigashima et al., 2021). NLGN3 gene was originally cloned from rat brains as a homolog of rat *Nlgn1* (Ichtchenko et al., 1996). *Nlgn3* is highly conserved from invertebrates to vertebrates including humans. *Nlgn3* is 32,272 bp in length on an X-chromosome region (Xq13.1) and composed of eight exons ranging from 60 to 1,864 bp (Philibert et al., 2000). The coding region spans from exon 2 to 8. Exons 7 and 8 are the largest exons, encoding about 65% of NLGN3 protein (Uchigashima et al., 2021) (**Figure II**). *Nlgn3* promotor has a Wnt signal-responsive element, allowing for Wnt-mediated transcriptional control of *Nlgn3* (Medina et al., 2018). *Nlgn3* contains four alternative splice variants (*Nlgn3*-A, +A1, +A2 and, +A1A2); the mature protein is made up of 848 amino acids in humans and rats and it is partly translated through postsynaptic local translational machinery (Ichtchenko et al., 1996; Philibert et al., 2000; Cajigas et al., 2012). From a structural point of view, NLGN3 is a single membrane spanning protein with a N-terminal hydrophobic sequence, a large extracellular domain, a highly conserved single transmembrane region, and a short cytoplasmic domain (Ichtchenko et al., 1996). The cholinesterase-like domain at the extracellular level has the α/β-hydrolase fold which is structurally shared with acetylcholinesterase and thyroglobulin (De Jaco et al., 2010). However, as for the other NLGNs isoforms, the α/β-hydrolase fold is commonly non-catalytic due to a lack of an active site serine and alternatively responsible for binding to other synaptic molecules.

Importantly, the extracellular cholinesterase-like domain also has the NLGN-NLGN dimerization interface which is highly conserved among different NLGNs isoforms (Dean et al., 2003; Arac et al., 2007; Yoshida et al., 2021). Indeed, NLGN3 molecule forms homodimers and heterodimers with other NLGNs isoforms in the secretory pathway and translocate to the plasma membrane (Poulopoulos et al., 2012; Yoshida et al., 2021). Although, NLGN3 is anatomically co-localized and biochemically co-immunoprecipitated with NLGN2 (Budreck nd Scheiffele, 2007) the heterodimer formation of NLGN2 and NLGN3 is still matter of debate. In situ chemical cross-linking study failed to detect heterodimers of NLGN2 and NLGN3 in hippocampal neurons (Poulopoulos et al., 2012). Moreover, Poulopoulos et al. reported that

the lack of dimerization retains NLGN3 in the secretory pathway while other groups reported that monomer mutants are able to translocate to the plasma membrane (Ko et al., 2009; Shipman and Nicoll, 2012b). Another important property of NLGN3 is its activity dependent cleavage: it can be cleaved on its juxtamembrane domain in an activity-dependent manner, which is conserved from rodents to humans (Bemben et al., 2019). A disintegrin and metalloproteinase domain-containing protein 10, also known as ADAM10 claves NLGN3 under basal condition while activity-dependent cleavage of NLGN3 is mediated by metabotropic glutamate receptor activation, protein kinase C (PKC) signaling, and matrix metalloproteinases (MMPs) (Kuhn et al., 2016; Venkatesh et al., 2017; Bemben et al.,2019). The extracellular domain of NLGN3 protein trans-synaptically binds to that of NRXNs in a Ca^{2+} dependent manner (Ichtchenko et al., 1996). In particular, all NLGN3 splice isoforms exhibit a higher binding affinity to β-NRXN without the insertion of AS4 than those with AS4 (Ichtchenko et al., 1996; Koehnke et al., 2010). It has been demonstrated that a specific trans-synaptic interaction between NLGN3-A and α-NRXN1+AS4 controls inhibitory synaptic transmission in an input cell-dependent manner (Uchigashima et al., 2020a). The short intracellular domain of NLGN3 contains the PDZ (Irie et al., 1997) and gephyrin-binding motifs (Poulopoulos et al., 2009). Notably, NLGN3 has some conserved phosphorylation sites in the intracellular domain but functional roles of NLGN3 phosphorylation sites remain unclear.

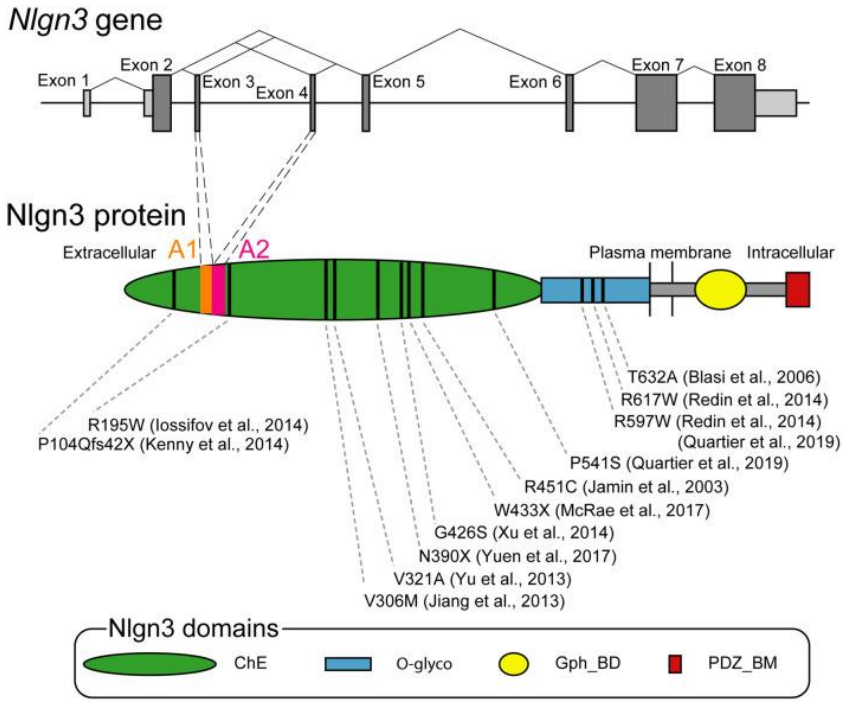

Figure II. *Genomic and protein structures of Neuroligin 3 (Uchigashima et al., 2021).*

NLGN3 expression

NLGN3 is expressed in neurons, astrocytes, oligodendrocyte precursor cells (OPCs), newly formed oligodendrocytes, and myelinating oligodendrocytes (Zhang et al., 2014; Proctor et al., 2015; Stogsdill et al., 2017). NLGN3 expression levels vary depending on the cell type, NLGN3 mRNA levels, for example, are significantly higher in D1 dopamine receptor expressing-MSNs (medium spiny neurons) than in D2-MSNs (Rothwell et al., 2014). Interestingly, the different splicing variants have different expression levels: NLGN3-A and NLGN3+A2 splice isoforms are dominantly expressed in hippocampal CA1 pyramidal cells (Uchigashima et al., 2020b). In mouse brain the expression levels are particularly high in the hippocampus, neocortex, striatum, and brain stem, and low in the thalamus and cerebellum.

NLGN3 function at synapses

To uncover the functional role of NLGN3 at synapses has been performed many studies based on overexpression, knockdown (KD), and KO of NLGN3 gene/protein. These experiments have revealed a complex picture in which NLGN3 can regulate synaptic function in an age, region, cell type and animal model-dependent manner. At excitatory synapses NLGN3 protein controls AMPAR-mediated basal excitatory transmission and its overexpression enhances AMPAR-mediated transmission together with the expression of presynaptic vesicular glutamate transporter 1 (VGLUT1) (Uchigashima et al., 2020b). However, global KO of NLGN3 gene results in no change in excitatory synaptic transmission (Foldy et al., 2013) or a small decrease in mEPSC frequency but not amplitude (Etherton M. et al., 2011). NLGN3 protein also contributes to NMDAR-mediated basal synaptic transmission at excitatory synapses on hippocampal CA1 inhibitory interneurons (Polepalli et al., 2017). In particular, the NLGN3 deletion in CA1 PV^+ inhibitory interneurons selectively causes a reduction in postsynaptic NMDAR-mediated synaptic transmission, but not in postsynaptic AMPAR-mediated synaptic currents. At inhibitory synapses in CA1 pyramidal neurons, global KO or P0 conditional KO of NLGN3 gene causes an increase in mIPSC frequency but not amplitude (Etherton M. et al., 2011; Jiang et al., 2017). In contrast, no change in either mIPSC amplitude or frequency was found in NLGN3 conditional KO mice at P21 (Jiang et al., 2017). Recent emerging studies have revealed that input cell-specific stimulation in NLGN3 KO mice shows a significant increase in synaptic strength at CCK^+ synapses, but no alteration at PV^+ synapses

(Foldy et al., 2013). The same authors proved that this selective strengthening of CCK^+ synapses is caused by disruption of tonic endocannabinoid signaling via cannabinoid CB1 receptors which are expressed at CCK^+ synapses. Moreover, in the nucleus accumbens, NLGN3 KO selectively reduces mIPSC frequency by 50% in D1-MSNs but not in D2-MSNs, consistent with cell type-specific expression of NLGN3 in D1-MSNs (Rothwell et al., 2014). Very few studies elucidate the role of NLGN3 protein in long-term synaptic plasticity. Zhang et al. (2015) showed no change in mGluR-mediated LTD in pan NLGN3-deficient Purkinje cells while Baudouin et al. (2012) reported that constitutive NLGN3 KO mice exhibited a loss of mGluR-mediated LTD. Interestingly, the same study show that NLGN3 KO mice exhibit ectopic climbing fiber synapses through heterosynaptic competition with parallel fiber synapses onto Purkinje cells (Baudouin et al., 2012) therefore causing abnormal remodeling of neuronal circuits. The functional importance of NLGN3 is also underlined by many studies in different brain regions. For example, NLGN3 KO cause the dysregulation of GluA2 lacking AMPAR insertion, which correlates with abnormal social behavior (Bariselli et al., 2018). In the hippocampus selective deletion of NLGN3 gene in PV^+ interneurons and NLGN3 KO mice display reduced power of gamma oscillations (Polepalli et al., 2017; Modi et al., 2019). Consistent with these impairments, PV^+ interneuron-specific NLGN3 KO mice exhibit abnormal hippocampus-dependent learning and memory, including fear memory retention and extinction (Polepalli et al., 2017). As demonstrated by the amount of studies focused on NLGN3, it is clear how this molecule can be a crucial molecular player in several non-syndromic monogenic form of ASD. Indeed, to date, over ten missense mutations have been identified on NLGN3 locus in individuals with ASD, thus identifying NLGN3 a privileged molecular target for the study of the complex pathophysiological determinants of ASD (Jamain et al., 2003; Blasi et al., 2006; Jiang et al., 2013; Yu et al., 2013; Iossifov et al., 2014; Kenny et al., 2014; Redin et al., 2014; Xu et al., 2014; Yuen et al., 2017; Quartier et al., 2019)

NLGN3 R451C mutation

In 2003, Jamain et al. conducted a study screening for NLGN3 and NLGN4Y mutations in 36 sibling pairs and 122 trios with autism or Asperger syndrome (AS). He found that in a Swedish family with two affected brothers, one with typical autism and the other with AS, a cytosine to thymine transition in NLGN3, inherited from the mother, changed a highly conserved arginine residue into cysteine (R451C) within the esterase domain. The estimated occurrence

of R451C mutation is < 3% among people with non-syndromic ASD (Quartier et al., 2019). A few years later its identification, the NLGN3 R451C point mutation has been introduced into the endogenous NLGN3 gene of mice using gene-targeting techniques (Tabuchi et al. 2007). One of the first observations was that R451C mutation site is located in the helix next to the NLGN3 dimerization interface and could be important for cell surface trafficking. Despite that, it has been showed that it does not interfere with dimerization of NLGN3 mutant protein (Poulopoulos et al., 2012), but shows retention of NLGN3 mutant in the endoplasmic reticulum (ER), leading to a 90% loss of NLGN3 from the cell surface (Chih et al., 2004; Comoletti et al., 2004). Additionally, another study showed that the mutant protein, retained in the ER, is preferentially degraded by the proteasome (Trobiani et al., 2018).

In 2007, Tabuchi et al. carried out an extensive functional characterization of NLGN3 R451C knockin (KI) mice with respect to NLGN3 knockout (KO) mice to test whether the R451C substitution represents a gain- or a loss-of-function change. These mutations did not cause global changes in the molecular composition of the brain, except for a small increase in inhibitory markers in the KI but not in the KO mice. In particular, the vesicular GABA transporter VGAT and the postsynaptic protein gephyrin were increased in the R451C KI mice whereas no change in VGAT levels were detected in the KO mice. Moreover, consistent with elevated expression of gephyrin and vesicular inhibitory amino acid transporter, in the somatosensory cortex, inhibitory synaptic transmission was significantly increased in NLGN3 R451C KI mice but not in NLGN3 KO mice (Tabuchi et al., 2007; Speed et al., 2015). Therefore, the autistic phenotype of the NLGN3 R451C KI mice is not due only to loss of function of GABAergic system. Concerning other brain regions, NLGN3 R451C KI mice exhibit a decrease in mIPSC amplitude in the basolateral amygdala (Hosie et al., 2018). Furthermore, in the nucleus accumbens, a reduction of mIPSC frequency on D1-MSNs is commonly observed in R451C KI mice and NLGN3 KO mice, consistent with cell type-specific expression of NLGN3 in D1-type medium spiny neurons (D1-MSNs) (Rothwell et al., 2014) suggesting a common dysfunction of striatal inhibitory circuits in both mutant mice.

Importantly, NLGN3 KO and NLGN3 R451C KI mice share specific impairments in tonic endocannabinoid signaling. Input cell-specific stimulation in NLGN3 KO mice shows a significant increase in synaptic strength at cholecystokinin (CCK^+) synapses, but no alteration at PV^+ synapses, suggesting an input cell dependent function of NLGN3 at hippocampal inhibitory synapses (Foldy et al., 2013). This selective strengthening of CCK^+ synapses, was also found in NLGN3 KI mice and it is caused by disruption of tonic endocannabinoid signaling via cannabinoid CB1 receptors which are expressed at CCK^+ synapses (Foldy et al., 2013).

Moreover, no change or a reduction in inhibitory transmission was found at either somatostatin (SST^+) synapses or parvalbumin (PV^+) synapses on pyramidal cells (Cellot and Cherubini, 2014; Speed et al., 2015).

At excitatory synapses NLGN3 KI mice exhibit a large increase in AMPAR-mediated excitatory synaptic transmission in the hippocampal CA1 region without any changes in presynaptic release probability and the expression of excitatory synaptic proteins (Etherton M. et al., 2011; Hosie et al., 2018). In addition, NLGN3 R451C KI mice also increase mEPSC frequency in Purkinje cells (Trobiani et al., 2018). NLGN3 protein also contributes to NMDAR mediated basal synaptic transmission at excitatory synapses on hippocampal CA1 inhibitory interneurons (Polepalli et al., 2017). It has been demonstrated that the R451C mutation can enhance NMDAR-mediated synaptic transmission, which may be partly caused by enhanced expression of GluN2B-containing receptors (Etherton M. et al., 2011). Despite these abnormalities, NLGN3 R451C missense mutations exhibit no major changes in hippocampal or cortical synapse size and density (Tabuchi et al., 2007; Etherton M. et al., 2011; Etherton M. R. et al., 2011). A few studies have investigated the impact of the R451C mutation on synaptic plasticity. NLGN3 R451C mutation significantly affects long-term synaptic plasticity with differential effects at distinct synapses. LTP is enhanced at hippocampal excitatory synapses (Etherton M. et al., 2011) while LTD is impaired at corticostriatal excitatory synapses (Martella et al., 2018).

NLGN3 R451C mutation can also affect the remodeling of neuronal circuits. In particular, in layer 2/3 of the somatosensory cortex KI mice show enhanced dynamics in spine expressing PSD95, which may be subsequently associated with stable synaptic connectivity (Isshiki et al., 2014) while in the cerebellum the mutation impairs elimination of redundant climbing fiber-Purkinje cell synapses from postnatal day 10–15 (Lai et al., 2021).

From the behavioral point of view NLGN3 KI line displayed impaired sociability, learning and memory (Etherton M. et al., 2011; Jaramillo et al., 2014). Other studies also found that NLGN3 R451C KI mice display increased repetitive behavior and aggressiveness, deficits in transitive inference, and abnormal wake and sleep EEG power spectral profiles (Burrows et al., 2015; Liu et al., 2017; Hosie et al., 2018; Norris et al., 2019). Rothwell et al. in 2014 observed that NLGN3 KI mice display enhanced rotarod performance and stereotypic behaviors which could be caused by the reduced inhibition found in D1-MSNs in the nucleus accumbens that regulates motor learning behavior.

Strikingly, different NLGN3 R451C KI lines have distinct sociability and learning and memory phenotypes (Tabuchi et al., 2007; Chadman et al., 2008). Indeed, it seems that behavioral differences are genetic background-dependent (Jaramillo et al., 2014, 2018), however, physiological properties of synapses are thought to be genetic background-independent (Etherton et al., 2011). In line with this, Etherton et al. in 2010 showed that two independently generated mouse lines exhibit the same phenotype: i) a large increase in AMPA and NMDA receptor-mediated excitatory synaptic transmission, ii) a dramatic change in NMDA receptor-mediated responses in the hippocampus, iii) an increase in inhibitory synaptic transmission in the somatosensory cortex. Therefore, NLGN3 R451C mutation induces circuit specific effect suggesting that the diverse clinical spectrum of ASD pathologies is secondary to region-specific susceptibilities that are probably modulated by genetic background effects and developmental or environmental influences (Etherton et al., 2011). Moreover, other factors, like housing environments, may also contribute to the inconsistent results between differen mouse line (Burrows et al., 2017, 2020; Kalbassi et al., 2017).

Lastly, it is worth to mention that a recent study on non-neuronal cell type showed that NLGN3 R451C mutation affects astrocytic morphology by reducing their branch point number, branch length, and territory in the dentate gyrus while the density of microglia is increased in the dentate gyrus of NLGN3 R451C KI mice (Matta et al., 2020). These data show that not only neurons but also other cell types can be affected by NLGN3 R451C mutation.

Therefore, from the evidence collected so far it seems clear that NLGN3 gene is strongly associated with a non-syndromic monogenic form of ASD. In particular, NLGN3 R451C mutation was proved to affect both inhibitory and excitatory transmission with distinct effects at different brain regions (see summary in **Table I**), cell types and synapses recapitulating the complex pathophysiological basis of ASD. In this concern, lot of works still need to be done to study for instance the role of plasticity, and in particular the interaction between excitatory and inhibitory plasticity, in ASD models. It could be also important to investigate dendritic function and network dynamics by exploiting calcium imaging and optogenetics or to test the effect of ASD-related mutation on the network with high throughput approaches such as electroencephalography (EEG).

Region	Synaptic defects	References
Hippocampus	Increased AMPAR-mediated excitatory synaptic transmission Enhanced NMDAR mediated synaptic transmission Enhanced expression of GluN2B-containing receptors Enhanced LTP at excitatory synapses	Etherton et al., 2011
	Enhanced synaptic transmission at Cck+ inhibitory synapses	Foldy et al., 2013
Cerebellum	Increased mEPSC frequency in Purkinje cells	Trobiani et al., 2018
	Impaired elimination of redundant climbing fiber-Purkinje cell synapses	Lai et al., 2021
Somatosensory cortex	Increased inhibitory synaptic transmission Elevated expression of gephyrin and VGAT Impaired endocannabinoid signalling at CB1-expressing Cck+ synapses	Tabuchi et al., 2007 - Speed et al., 2015
	Abnormal PSD 95+ spine dynamics	Isshiki et al., 2014
	Reduction of inhibitory transmission at PV+ synapses on PC cells	Cellot and Cherubini, 2014 - Speed et al., 2015
Basolateral amygdala	Increased excitatory transmission Decreased mIPSC amplitude	Hosie et al., 2018
Nucleus accumbens	Reduction of mIPSC frequency on D1-MSNs	Rothwell et al., 2014
Dorsal striatum	Impaired LTD at excitatory synapses	Martella et al., 2018

***Table I**. Summary of synaptic impairments found in NLGN3 R451C KI mouse.*

AIM OF THE WORK

Previous work showed impaired excitation to inhibition ratio (E/I) in mice carrying the ASD-associated R451C point mutation on the NLGN3 gene. However more recent studies have posed the important question of whether the altered E/I ratio is the cause of ASD or rather represents homeostatic (although insufficient) mechanism aimed at keeping constant the neuronal firing (Antoine et al., 2019).

Our main hypothesis is that the **altered E/I ratio in NLGN3 R451C KI mice impairs the synaptic dynamic range, that is modulated by synaptic plasticity in wild type synapses, thus preventing the correct network remodeling following external inputs**.

To this aim, we employed different experimental approaches including single molecule tracking, quantitative immunocytochemistry, laser neurotransmitter photolysis and electrophysiology to study basal and activity-dependent glutamatergic and GABAergic synaptic transmission in NLGN3 R451C KI and WT neurons.

The present thesis analyzes two main aspects of synaptic excitation and inhibition in response to chemical plasticity-inducing protocol:

1. Organization and dynamics of synaptic proteins

In this framework in both WT and NLGN3 R451C KI mice we studied the synaptic localization and the dynamics of different synaptic proteins such as NLGN3, NMDA receptors (containing the GluN1 and GluN2 subunits), AMPA receptors, gephyrin, GABAA receptors (containing both the α1 and α2 subunits). We found that, the loss of NLGN3 at NLGN3 R45C KI synapses induced an overall destabilization of the synaptic organization.

2. Study of excitatory and inhibitory synaptic currents

In order to investigate the synaptic function in WT and NLGN3 R451C KI mice we recorded both spontaneous excitatory and inhibitory currents (sEPSCs, sIPSCs) from primary neuronal cultures. These experiments allowed to functionally corroborate the data obtained in experiments as described in point 1. In addition, experiments aimed at eliciting synaptic-like currents with the laser uncaging technique (uEPSCs, uIPSCs), confirmed that the plasticity observed in WT mice and the altered plasticity in NLGN3 R451C KI mice are due to postsynaptic mechanisms.

Overall, the present work aims at providing an insight into the role of the coordinated excitatory and inhibitory synaptic plasticity, highlighting that the dysregulation of the activity-dependent modification of synaptic strength may represent an important determinant for ASD pathophysiology.

RESULTS

1. Reduced surface expression and enhanced later diffusion of NLGN3 R451C at inhibitory synapses

In a first set of experiments, we assessed by immunocytochemistry the effects of the R451C point mutation on the surface expression of NLGN3. Since antibodies recognizing the extracellular domain of NLGN3 protein with satisfactory specificity are not available, we inserted a HA tag in the extracellular domain of both the WT and NLGN3 R451C (KI) proteins and expressed them in hippocampal cultures obtained from WT and NLGN3 KI mice, respectively. This allowed us to immunolabel NLGN3 surface expression by using anti-HA antibodies. In line with previous quantitative immunoblotting data showing that NLGN3-KI is less expressed by ~90% in mouse forebrain (Tabuchi et al., 2007), we found that in NLGN3 KI hippocampal cultures, the total surface expression of NLGN3 was reduced by ~95% as compared to NLGN3 WT neurons. (WT: n=20, KI: n=14; $p<0.0001$, t-test; Figure 1A e B).

Next, we investigated whether the R451C point mutation merely reduced the surface availability of NLGN3 molecules or also altered their intrinsic properties such as the lateral mobility. To this purpose we studied the diffusion of surface NLGN3 by single particle tracking. Again, we exploited anti HA antibodies (in this case coupled to individual quantum dots) to pinpoint NLGN3 WT-HA and NLGN3 KI-HA in WT and KI hippocampal cultures, respectively. We discriminated and analysed separately the trajectories of NLGN3-HA-QD complexes exploring excitatory or inhibitory synapses. In these experiments we identified excitatory synapses by transfecting cultured neurons with Homer-GFP (not shown), a scaffold protein of the glutamatergic post-synaptic density (PSD), and inhibitory synapses by live labeling of the presynaptic marker vGAT (as in Ravasenga et al., 2021) (Figure 1C). Interestingly, we observed that the mutation significantly increased the mobility of NLGN3 KI-HA at inhibitory synapses as compared to NLGN3 WT-HA, as indicated by larger diffusion coefficient values (n= 296 and n= 200, $p<0.001$, Mann-Whitney test, Figure 1D left). In line with this, the fraction of immobile NLGN3 molecules at inhibitory synapses was smaller in NLGN3 KI neurons than in NLGN3 WT neurons (n= 200 and n= 298, $p<0.001$, t- test; Figure 1D right). Moreover, we observed a decreased confinement of NLGN3 KI-HA at inhibitory synapses as suggested by the higher steady state of the mean square displacement (MSD) curve as compared to WT conditions ($F_{1, 6129}=343.7$; two-way ANOVA, $p<0.0001$ Figure 1E).

We then looked at the mobility of NLGN3 WT-HA and NLGN3 KI-HA at excitatory synapses. Here, the lateral diffusion of NLGN3-HA molecules was comparable between the two genotypes (n=299 and n=232, p=0.814, Mann-Whitney test, Figure 1F left) and, in line with this, the fraction of immobile NLGN3 molecules didn't show any difference between WT and KI neurons (n=299 and n=232 respectively, p=0.712, t-test; Figure 1F right). Accordingly, at excitatory synapses the MSD curve of NLGN3 KI molecules was comparable with that of WT molecules ($F_{1, 5781}=3.12$; two-way ANOVA, p=0.077, Figure 1G).

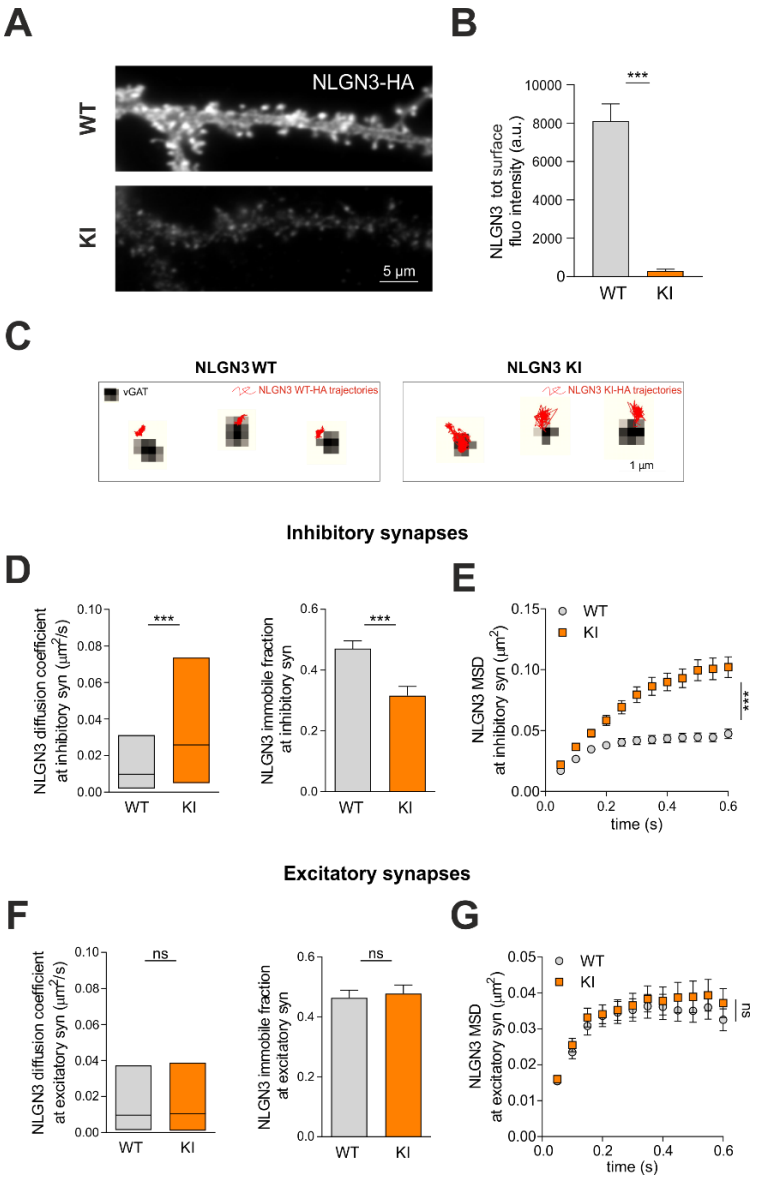

Figure 1. Characterization of NLGN3 surface expression and diffusion properties at excitatory and inhibitory synapses. (A) Representative micrographs of HA surface immunoreactivity in primary hippocampal cultures from NLGN3 WT and KI mice transfected with HA-tagged NLGN3-WT or -KI plasmids, respectively. Scale bar, 5 µm. **(B)** Quantification of NLGN3-HA average fluorescence intensity detected in total neuronal surface of NLGN3 WT and KI mice. In NLGN3 KI neurons surface NLGN3 KI-HA is poorly expressed as compared to WT. **(C)** Example trajectories of NLGN3-HA diffusing on NLGN3 WT and KI neurons. Again, the HA-tagged WT and KI constructs were overexpressed in WT and KI cultures, respectively. Inhibitory synapses, identified through VGAT immunolabeling, are represented in gray scale. Scale bar, 1 µm. **(D, F)** Quantification of the diffusion coefficient and immobile fraction of NLGN3-HA in NLGN3 WT and KI neurons at inhibitory (D) and excitatory (F) synapses. Please note that, the larger diffusion coefficient value and the smaller fraction of immobile NLGN3 KI molecules at inhibitory synapses indicate that the mutated NLGN3 shows higher mobility compare to the NLGN3 WT, while there are no significant differences in the behaviour of the NLGN3 KI at excitatory synapses. **(E, G)** Quantification of the mean square displacement (MSD) of NLGN3-HA WT and KI at inhibitory (E) and excitatory (G) synapses. In line with the results showed in D and F, the mean square displacement (proportional to the area explored by the NLGN3 molecules at synapses) was significantly higher at NLGN3 KI inhibitory synapses as compared to the WT with no changes at excitatory synapses. Values are expressed as mean ± SEM and as median ± IQR. ***p < 0.001, ns = not significant.

2. Increased lateral mobility of synaptic GABAAR in NLGN3 KI neurons

Since the alterations of NLGN3 KI lateral mobility were mainly observed at inhibitory synapses, we further investigated whether this effect could also influence the dynamics of other synaptic components, such as GABAA receptors. The lateral mobility of individual α1 or α2 subunit- containing GABAARs was assessed in 1-minute-long movies by labeling the receptors with QDs by means of specific primary antibodies. Overall, in KI cultures the lateral diffusion of the α1 and α2 subunits of GABAA receptors was significantly increased with respect to WT. Indeed, we measured higher diffusion coefficients of α1- and α2-containing GABAARs in NLGN3 R451C KI neurons as compared to the WT counterparts (α1: n= 683 (WT) and 894 (KI), Mann-Whitney test, $p<0.0001$, Figure 2B left; α2: n= 192 (WT) and 173 (KI), $p<0.01$ Figure 2D left). As supporting evidence of increased mobility of α1- and α2-GABAARs, the fraction of the receptors trapped at the inhibitory synapses was only 0.36±0.01 in NLGN3 R451C KI vs 0.42±0.02 in WT cultures for α1 subunit (n=894 and 683, in KI and WT respectively t-test; p=0.014; Figure 2B right) and 0.24 ±0.03 vs 0.34±0.03 for α2, respectively (n=173 and 192, in KI and WT respectively, t-test; p=0.034; Figure 2D right). Moreover, the mean square displacement (MSD) versus time curves, which provide a reliable estimation of receptor confinement at synapses, exhibit higher initial slope and steady state values in NLGN3 KI with respect to the WT, indicating that the mutation determines lower confinement of both α1- and α2-containing GABAAR at inhibitory synapses (α1: $F_{1,21487} = 310.2$; two-way ANOVA, $p<0.0001$; α2: $F_{1,6772} = 70.85$; two-way ANOVA, $p<0.0001$ Figure 2C and 2E, respectively). These data suggest that the global increase of the lateral mobility is due to a strong reduction in the fraction of immobile receptors at synapses as well as intrinsic changes in the diffusive properties of mobile receptor population. Overall, those data point towards a destabilization of GABAA receptors at inhibitory synapses induced by the presence of the mutated NLGN3 concomitant to its reduced surface availability.

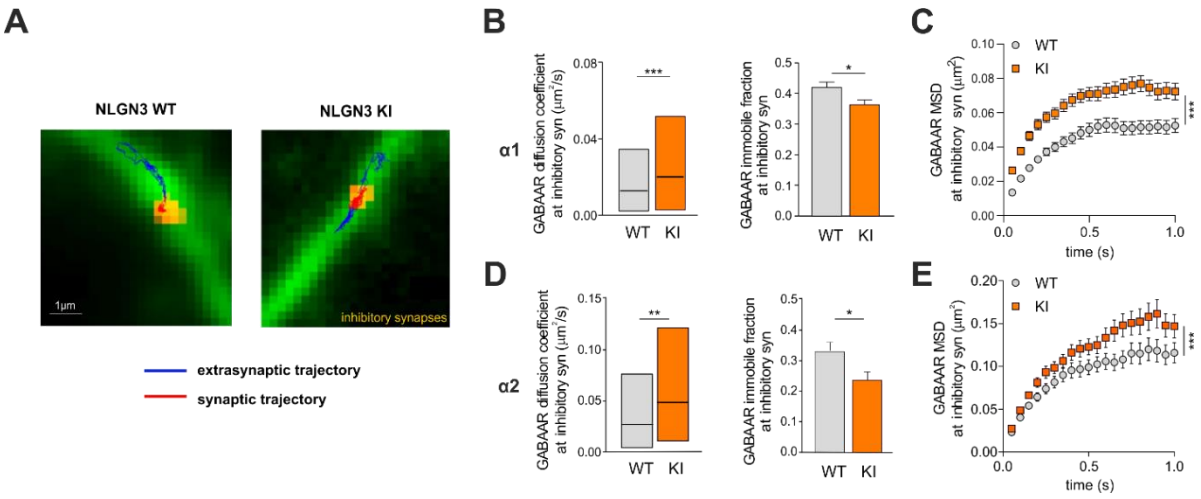

Figure 2. Increased surface GABAAR lateral diffusion at inhibitory synapses in NLGN3 KI neurons as compared to WT. (A) Example trajectories of extrasynaptic (blu) and synaptic (red) α1 subunit of GABAARs diffusing on NLGN3 WT and KI neurons. Inhibitory synapses are represented in yellow. Scale bar, 1 µm. **(B, D)** Quantification of the diffusion coefficient (median ± IQR). (**C, E**) Quantification of the mean square displacement (MSD) of α1 (C) and α2 (E) subunit of GABAAR in WT and NLGN3 KI neurons. Unless otherwise stated, values are expressed as mean ± SEM.*p < 0.05, **p < 0.01, ***p < 0.001, ns = not significant.

3. NLGN3 R451C does not affect spontaneous synaptic transmission

To further investigate the impact of the R451C mutation on the basal neuronal activity, we performed electrophysiological recordings using the patch clamp technique in the whole-cell configuration. At inhibitory synapses, where GABAA receptors lateral mobility is altered in NLGN3 KI conditions, we recorded the spontaneous inhibitory postsynaptic currents (sIPSC) from NLGN3 WT and NLGN3 KI cultured hippocampal neurons (Figure 3A). sIPSC from WT and KI neurons showed comparable amplitude (WT: n=33, KI: n=23, p=0.100, t-test; Figure 3B left). Similarly, when we recorded spontaneous excitatory postsynaptic currents (sEPSC) in WT and KI neurons (Figure 3C) we did not observe any significant difference in currents amplitude (n=7 and n=11, p=0.876, t-test; Figure 3D left). So far, the experiments suggest that, in basal conditions, the mild postsynaptic alterations induced by the NLGN3-R451C mutation do not affect spontaneous synaptic transmission.

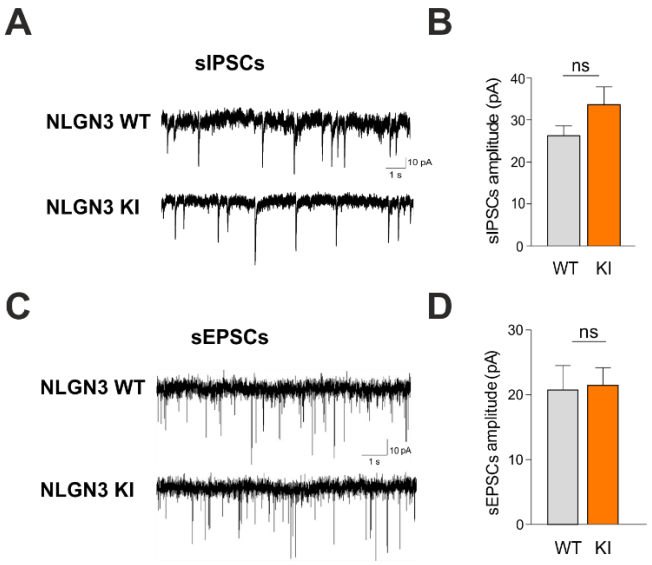

Figure 3. NLGN3 R451C mutation does not affect basal synaptic transmission. (A, C) Example electrophysiology traces of sIPSCs (A) and sEPSCs (C) recorded in NLGN3 WT (upper trace) and NLGN3 KI (lower trace) neurons. **(B, D)** Quantification of sIPSC (B) and sEPSCs (D) amplitude in WT and KI neurons. Please note that both excitatory and inhibitory synaptic currents in KI neurons are comparable to those in WT neurons. Values are expressed as mean ± SEM. ns = not significant.

4. NLGN3 surface expression and lateral mobility upon induction of synaptic plasticity

Next, we hypothesized that in basal conditions the effects of the genetic alterations of NLGN3 R451C could be mildly detectable due to poor neuronal activity. We reasoned that, on the contrary, some sizable effects might be unmasked in response of external stimuli able to induce synaptic plasticity. Following this hypothesis, we addressed whether the NLGN3 R451C mutation could interfere with the expression of synaptic plasticity. We adopted a previously published chemical protocol for plasticity based on a brief application of NMDA, able to induce long term depression (LTD) at glutamatergic synapses and concomitantly long-term potentiation at GABAergic synapses (iLTP) (Marsden et al., 2007; Petrini et al., 2014). The stimulation consisted of incubating hippocampal cultured neurons with NMDA+CNQX for 2 minutes and allowing at least 20 minutes of recovery before monitoring the effects. In a first set of experiments, we aimed at understanding whether the surface levels of NLGN3 protein were affected by the induction of synaptic plasticity. We applied the NMDA-based plasticity protocol (or a sham) both to WT and NLGN3 KI cultures transfected with NLGN3 WT-HA or NLGN3 R451C-HA constructs, respectively and we immunoprobed the HA tag. Among WT neurons, NMDA-treated samples showed remarkably less NLGN3 immunoreactivity as compared to sham-treated samples (NLGN3 total average fluorescence intensity: sham n=20;

NMDA n=29, p= 0.006, t-test; Figure 4A-B). In contrast, the poor immunoreactivity detected in NLGN3 KI neurons remained unchanged upon NMDA stimulation (NLGN3 R451C average fluorescence intensity: sham: n=14; NMDA: n=13, p=0.169, t-test; Figure 4A-4B) suggesting that NLGN3 KI mice present altered expression of surface NLGN3 after the induction of the plasticity protocol.

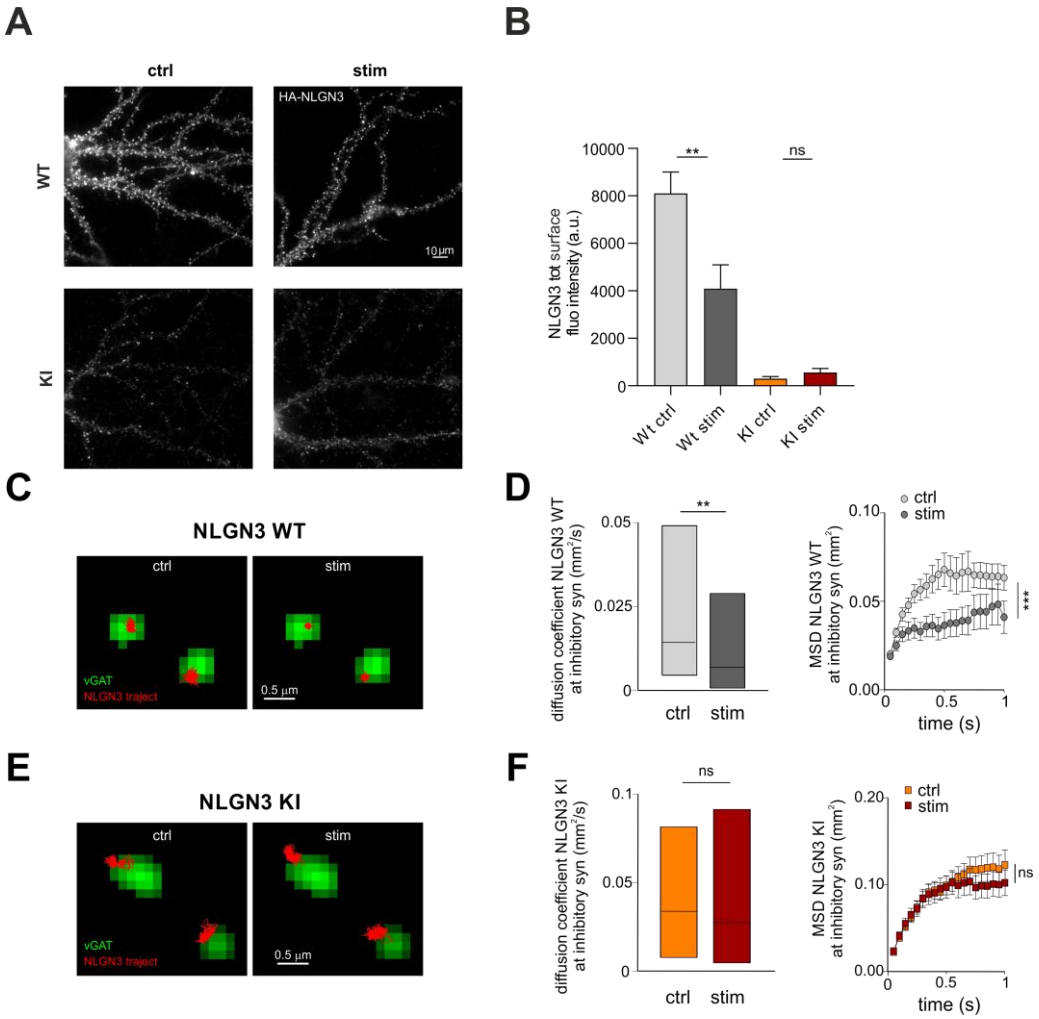

Figure 4. Effect of the NMDA stimulation on NLGN3-HA surface expression and mobility at inhibitory synapses in WT and KI neurons. (A) Representative micrographs of total surface NLGN3-HA immunoreactivity upon sham (ctrl) or NMDA stimulation (stim) in NLGN3 WT and KI mice. Note that the NLGN3 WT-HA and the NLGN3 KI-HA constructs were transfected in NLGN3 WT and the NLGN3 KI neurons, respectively. Scale bar, 10 µm. **(B)** Quantification of NLGN3 total average immunoreactivity in the immunocytochemistry experiment described in A. Please note that, in WT conditions, NMDA treatment significantly decreased NLGN3 total surface fluorescence intensity. In contrast, in KI mice, NLGN3 intensity was comparable before and after NMDA treatment. **(C, E)** Example trajectories of recombinant NLGN3-HA protein (red) diffusing at inhibitory synapses, identified by vGAT clusters (green), at WT (C) and KI (E) neurons. Scale bar, 0.5 µm. **(D, F)** Quantification of the diffusion coefficient (median ± IQR) and mean square displacement (MSD) of NLGN3 protein at inhibitory synapses in WT (D) and KI neurons (F). Unless otherwise stated, values are expressed as mean ± SEM. **p < 0.01, ***p < 0.001, ns = not significant.

Next, we aimed at assessing the effects of the plasticity protocol on the lateral mobility of NLGN3 in WT and KI neuronal cultures. In analogy to the experimental approach applied in basal conditions, we probed the lateral diffusion of individual HA-tagged NLGN3 molecules (either WT or carrying the R451C mutation) by using anti-HA antibodies coupled to QDs. Again, inhibitory synapses were localized by live labeling of vGAT (see methods) (Figure 4C-4E). We monitored NLGN3 mobility on the same samples, before and 20 min after NMDA stimulation. In WT neurons, after NMDA treatment, we observed an overall significant immobilization of NLGN3-HA WT diffusion at inhibitory synapses as quantified by a significant reduction of the median diffusion coefficient (n=185 before and 65 after; p=0.005, Mann-Whitney; Figure 4D right) and an increased confinement suggested by a lower MSD curve ($F_{1,4474}$=62.72; p<0.0001, Two Way ANOVA; Figure 4D left). On the contrary, the mobility of NLGN3 KI was not affected by NMDA stimulation. At inhibitory synapse both the diffusion coefficient and the MSD curve were comparable before and after the stimulation protocol (diffusion: n=85 before and 60 after; p=0.880, Mann-Whitney; MSD: $F_{1,2526}$=3.50; p=0.0614; Two Way ANOVA; Figure 4F).

5. Lack of iLTP in NLGN3 KI neurons

As a next step to dissect how NLGN3 KI neurons respond to the induction of synaptic plasticity we recorded spontaneous inhibitory post-synaptic currents (sIPSCs) before and after the stimulation with NMDA with electrophysiological experiments using the patch clamp technique in the whole-cell configuration (Figure 5A). In line with the literature (Marsden 2007, Petrini 2014), in WT neurons, spontaneous inhibitory synaptic currents (sIPSCs) recorded before and over time after the NMDA treatment showed a persistent increase in their amplitude (n=28; F3,81= 2.88; p=0.041, RM one-way ANOVA; Figure 5B left) which lasted for more than 30 min (p=0.034 after 30 min, paired t-test; Figure 5B left inset). On the contrary, in NLGN3 KI neurons, the amplitude of sIPSCs remained stable over time (n=17; F3,64= 0.29; p=0.827, RM one-way ANOVA; Figure 5B right) and did not show statistically significant difference after 30 min as compared to before the treatment (p=0.466 after 30 min; paired t-test; Figure 5B right inset).

Since the number of receptors available at the postsynaptic sites are crucial to determine the strength of synaptic transmission, we next investigated whether the lack of expression of iLTP

in NLGN3 KI neurons correlated with GABAA receptor availability at synapses upon stimulation. We immunoprobed PFA-fixed samples 20 minutes after the delivery of NMDA protocol or a sham, to immunolabel α1 and α2 subunits of GABAAR (Figure 5C-5E). In WT neurons, quantitative analysis showed a significantly larger GABAAR fluorescence intensity detected at the total neuronal surface and at synaptic clusters in stimulated samples as compared to controls (α1: sham n=89, NMDA n=104, p=0.002 and p=0.021 respectively, t-test, Figure 5D), (α2: sham n=63, NMDA n=57, p=0.011 and p=0.005, respectively, t-test, Figure 5F). In contrast, in NLGN3 KI cultures, the same chemical protocol did not induce any change in the total surface and synaptic clusters intensity of the α1 subunit (sham n=91, NMDA n=91, p=0.192 and p=0.203 respectively, t-test, Figure 5D), and of the α2 (sham n=71, NMDA n=64, p=0.498 and p=0.676, t-test, Figure 5F), in line with the lack of iLTP. As a side note, we detected larger α2 immunoreactivity in NLGN3 KI cells both at the total neuronal surface and at synaptic clusters compared to WT cells (WT: n=63 and KI: n= 71, t-test, p=0.0004 and p=0.015 respectively, Figure 5F) suggesting an up-regulation of α2 subunit in the mutant mice. In another set of experiments we also checked whether gephyrin reorganization at inhibitory synapses, another mechanism underlying the expression of iLTP (Petrini et al 2014, Pennacchietti et al. 2017), was lacking in NLGN3 KI neurons after NMDA treatment (Figure 5G). As expected, both gephyrin total and synaptic fluorescence intensity were comparable in NLGN3 KI neurons (sham: n=52, NMDA: n=58, p=0.361 and p=0.732 respectively, t-test; Figure 5H), whereas they were significantly increased in NLGN3 WT cultures (sham n=49, NMDA n=47, p<0.0001 and p=0.019 respectively, t-test; Figure 5H).

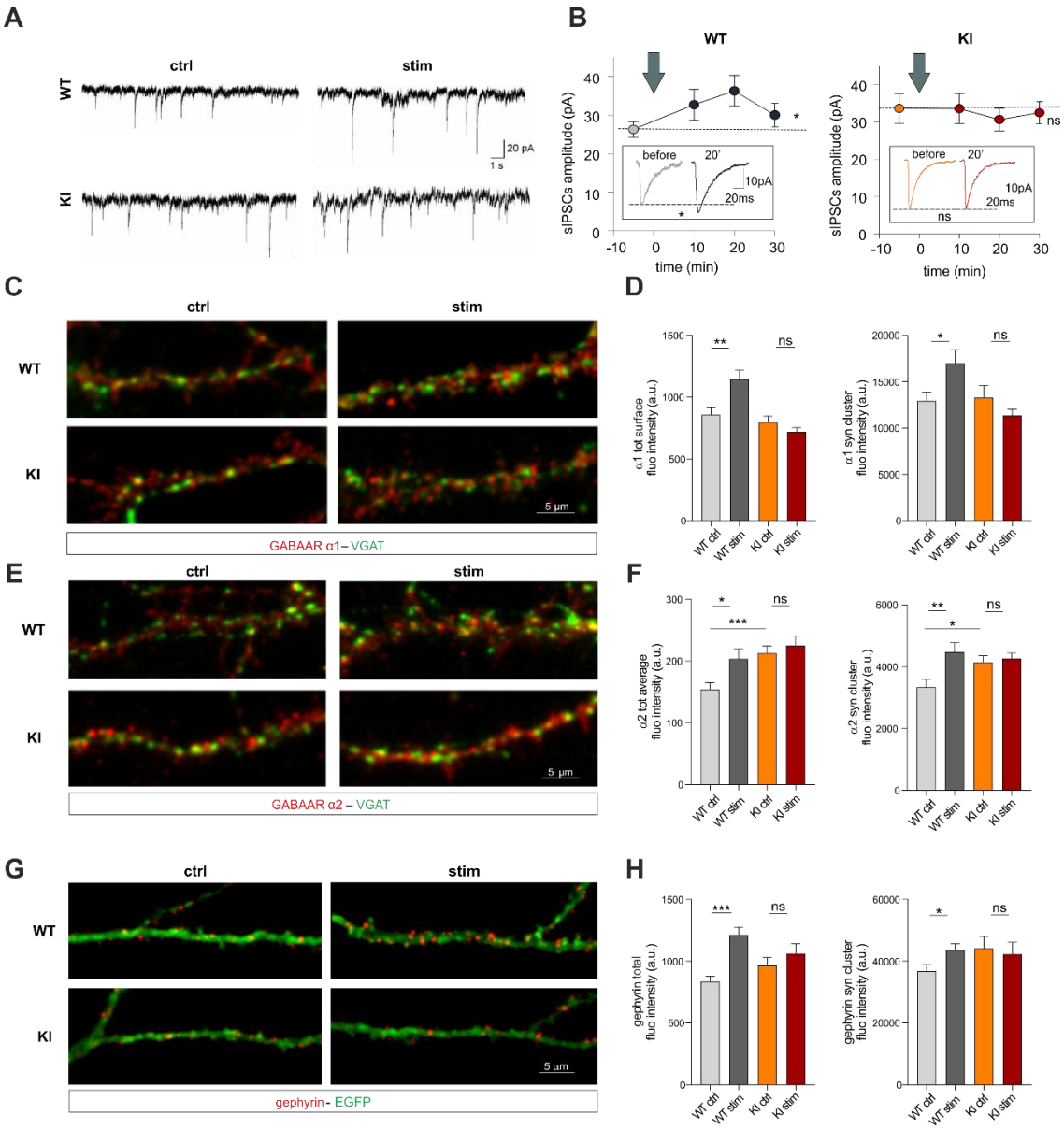

Figure 5. Long-term potentiation of inhibitory synaptic transmission is impaired in neurons from NLGN3 KI mice. (A) Representative patch-clamp recordings of spontaneous inhibitory postsynaptic currents (sIPSCs) acquired before and 20 min after the NMDA stimulation in NLGN3 WT (upper trace) and NLGN3 KI (lower trace) neurons.. **(B)** Time course of sIPSCs amplitude before and after NMDA treatment in WT (left panel) and NLGN3 KI cultures (right panel). Insets: example of averaged sIPSCs current before and 20 min after the plasticity induction for WT (left panel) and NLGN3 KI (right panel). Please note that after NMDA application, WT currents show a progressive amplitude increase indicating the expression of iLTP, whereas NLGN3 KI currents remained unchanged. **(C, E)** Representative multicolor images of GABAAR immunoreactivity (red) (the α1 subunit is shown in C and the α2 subunit is shown in E) along with V-GAT (green), from NLGN3 WT and KI mice treated with a sham (ctrl) or a NMDA solution (stim). Scale bar, 5 µm. **(D, F)** Quantification of total average fluorescence intensity and synaptic clusters intensity of α1 (D) and α2 (F) in ctrl and NMDA conditions in NLGN3 WT and KI neuron. **(G)** Representative images of gephyrin immunostaining (red) in EGFP-transfected neurons (green) from NLGN3 WT and KI mice treated with a sham (ctrl) or a NMDA treatment (stim). Scale bar, 5 µm. **(H)** Quantification of the total average fluorescence intensity (left) and synaptic clusters intensity (right) of gephyrin in WT and KI. Please note that, in KI conditions, NMDA failed to increase α1, α2 and gephyrin fluorescence. Values are expressed as mean ± SEM.*p < 0.05, **p < 0.01, ***p < 0.001, ns = not significant.

The results on WT neurons are in line with a previous study from our lab indicating that NMDA-induced iLTP relies on the accumulation of both GABAARs and the scaffold protein gephyrin at synapses (Petrini et al., 2014). The present data show that the mechanisms that allow the expression of iLTP are impaired in NLGN3 KI neurons.

6. Lack of LTD in NLGN3 KI neurons

Since the plasticity protocol based on a brief application of NMDA is also able to induce LTD at glutamatergic synapses, we next studied the plasticity of excitatory synapses in both NLGN3 WT and KI neurons. In WT neurons we observed a progressive reduction of sEPSCs amplitude over time (n=7, $F_{3,18} = 5.97$; $p = 0.005$; RM one way ANOVA; Figure 6B left) up to 30 min after the stimulus ($p=0.024$ after 30 min, paired t-test; Figure 6B left inset) indicating the long-term depression (LTD) of glutamatergic excitatory synapses. On the contrary, in NLGN3 KI neurons, the amplitude of sEPSCs did not show significant variations over time after the delivery of the NMDA protocol (n=11; $F_{3,30} = 1.28$; $p = 0.299$; RM one way ANOVA; Figure 6B right) up to 30 minutes ($p=0.155$, paired t-test, Figure 6B right inset), suggesting that NLGN3 mutant mice exhibit impaired excitatory synaptic plasticity in hippocampal neurons.

In analogy with the study at inhibitory synapses, in order to assess the correlation between expression of synaptic plasticity and receptor synaptic availability, we probed surface GluA1- and GluA2-containing AMPA receptors by immunocytochemistry. Excitatory synapses were concomitantly visualized by Homer1C-GFP fluorescence (Figure 6C-6E). In line with previous data (He et al., 2011; Lee et al., 1998), during the expression of NMDA-induced LTD we observed that in WT neurons, GluA1 and GluA2 subunit expression was reduced at glutamatergic synapses. In particular, the total surface fluorescence intensity and the synaptic clusters fluorescence intensity of GluA1 were considerably decreased after the application of the plasticity protocol (sham: n=68, NMDA: n=73; total surface fluorescence intensity: $p=0.034$, t-test, synaptic clusters fluorescence intensity: $p=0.0005$ t-test, Figure 6D). Similarly, GluA2 total surface fluorescence intensity was decreased in WT cells after the NMDA protocol (sham: n=90, NMDA: n=91, $p=0.026$, t-test, Figure 6F left) while synaptic clusters fluorescence intensity showed only a trend for reduction although it didn't reach statistical significance (sham: n=90, NMDA: n=91, $p=0.275$, t-test, Figure 6F right). On the contrary, in NLGN3 KI neurons, neither the total surface fluorescence intensity nor the synaptic content of

GluA1 and GluA2 were affected by NMDA treatment (GluA1: sham n=77, NMDA n=78, p=0.909 and p=0.710, t-test, Figure 6D; GluA2: sham n=97, NMDA n=90, p=0.252 and p=0.733, t-test, Figure 6F), supporting the evidence that excitatory synaptic strength was not affected by NMDA stimulation in NLGN3 KI neurons.

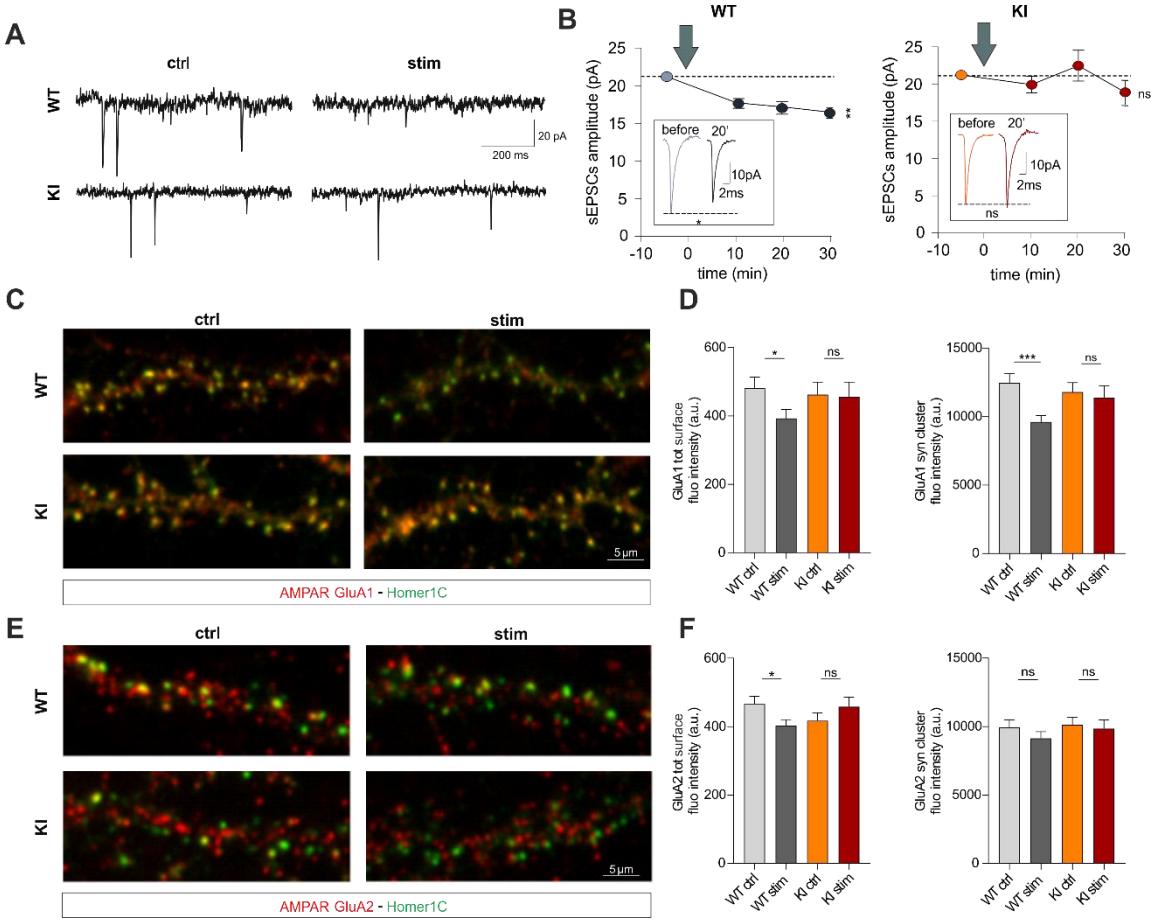

Figure 6. **The NLGN3 R451C mutation in KI mice prevents LTD expression. (A)** Example electrophysiology traces of spontaneous excitatory postsynaptic currents (sEPSCs) acquired before and 20 min after the induction of LTD NLGN3 WT (upper trace) and NLGN3 KI (lower trace) neurons. **(B)** Summary of sEPSCs amplitude over time recorded before and after the application of the NMDA in WT (left panel) and NLGN3 KI cultures (right panel). Please note that after NMDA treatment in WT neurons, synaptic currents show a progressive amplitude reduction indicating the expression of LTD whereas in NLGN3 KI neurons, current amplitude remained unchanged. Insets: examples of averaged sEPSCs before and 20 min after stimulation in WT (left panel) and NLGN3 KI cells (right panel). **(C, E)** Representative images of the immunolabeling of GluA1 and GluA2 subunits (red) of AMPA receptor in cultures from WT (upper panels) and NLGN3 KI (lower panels) mice, transfected with homer1C-GFP (green), treated with a sham (ctrl) or the NMDA solution (stim). Scale bar, 5 µm. **(D, F)** Quantification of GluA1 (D) and GluA2 (F) total average fluorescence intensity and synaptic clusters intensity in control and NMDA conditions. Please note that, in WT neurons, NMDA treatment decreased GluA1 and GluA2 total fluorescence intensity. In contrast, in NLGN3 KI cells, Glu1A and $p < 0.01$, ***$p < 0.001$, ns = not significant.

All together, these experiments showed that NLGN3 R451C mutation prevents the expression of LTD by interfering with the mechanisms that would lead the reduction of synaptic AMPA receptors upon NMDA stimulation.

7. NLGN3 KI neurons altered plasticity at single synapse level

Since the NMDA-based plasticity protocol has been demonstrated to be primarily due to changes at the postsynaptic level, we aimed at directly supporting this notion by eliciting postsynaptic responses with the uncaging technique instead of the activation of presynaptic terminals. This technique consists in the photorelease of caged neurotransmitters (NTs) in diffraction-limited spots. Briefly, the NT is covalently bound to a chemical "cage" that prevents its binding to its specific receptor. Following light illumination at appropriate wavelength, the NT is released from its cage, and becomes free to bind the receptor, leading to a current flow. The possibility to shed light in a restrained area (~ 500 nm diameter) represents a technical advantage that allows the selective activation of a single synapse. In a first set of experiments, we exploited this technique using the caged glutamate "MNI-Glutamate", combined with electrophysiology, to elicit uncaged excitatory postsynaptic currents (uEPSCs) from individual glutamatergic synapses in NLGN3 WT and KI neurons. Excitatory synapses were identified in hippocampal cultures by recombinant Homer1C-DsRed fluorescence (see methods) (Figure 7A). In line with sIPSCs recordings, this approach confirmed that NLGN3 R451C mutation does not alter basal synaptic responses, as we observed uEPSCs of comparable amplitude in NLGN3 WT and NLGN3 KI neurons (n=18 and n=22 respectively, p=0.853, t-test; Figure 7B). We next monitored the amplitude of uEPSCs before and after the NMDA stimulation to isolate a pure postsynaptic expression of synaptic plasticity (Figure 7C). In NLGN3 WT neurons, NMDA induced a decrease of the uEPSCs amplitude, indicating LTD expression, (n= 18, t-test, $p<0.0001$ 15 min after NMDA stimulation, Wilcoxon test; Figure 7D). On the contrary, in NLGN3 KI cultures, the same protocol was not able to induce LTD, being the uEPSCs comparable before and after the application of NMDA (n=22, p=0.750 15 min after NMDA stimulation, Wilcoxon test; Figure 7D).

With a similar approach, we next focused on the inhibitory counterpart. Uncaged inhibitory postsynaptic currents (uIPSCs) were elicited by photoreleasing DPNI-Gaba at inhibitory synapses visualized by gephyrin-EGFP fluorescence (see methods) (Figure 7E). In basal conditions, we did not quantify significant differences in the amplitude of uIPSCs between WT

and KI neurons (n=54 and n=70 respectively, p=0.765, t-test; Figure 7F). Next we studied NMDA-induced synaptic plasticity. In NLGN3 WT neurons, the application of the NMDA protocol elicited an increase of uIPSCs amplitude (Figure 7G), indicating the expression of iLTP (n=14, p<0.0001 15 min after NMDA stimulation, Wilcoxon test; Figure 7H) consistent with sIPSCs recordings. On the contrary, in the presence of the R451C mutation, not only did the NMDA stimulation fail to induce iLTP, but even it reduced the amplitude of uIPSCs indicating iLTD (n=19, p<0.0001 15 min after NMDA stimulation, Wilcoxon test; Figure 7H right).

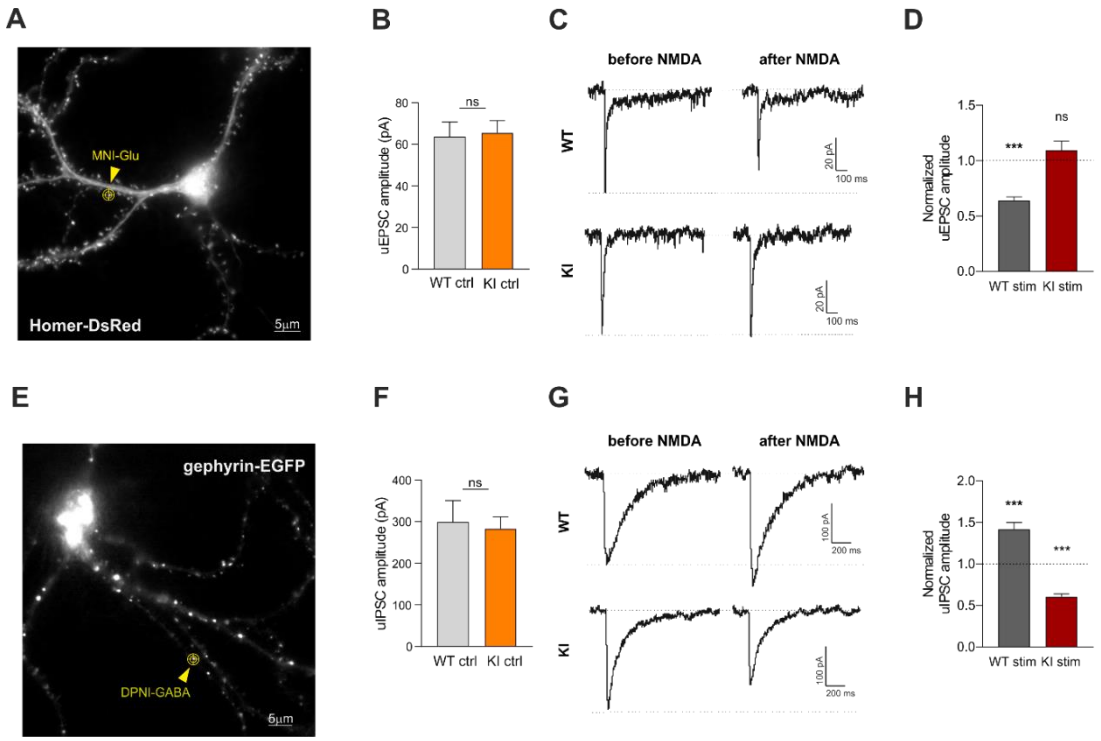

Figure 7. Impaired plasticity in NLGN3 KI excitatory and inhibitory currents evoked exploiting the uncaging technique se. (A,E) Representative micrographs of a Homer-DsRed expressing neuron (A) and gephyrin-GFP expressing neuron (E) for the identification of glutamatergic spines and GABAergic synapses respectively. The target symbol indicates an individual synapse where a diffraction-limited 378 nm UV laser spot was directed to uncage MNI-glutamate or DPNI-GABA. Scale bar, 5 µm. **(B, F)** Quantification of uEPSCs (B) and uIPSC (F) amplitude recorded from WT and KI neurons in basal conditions indicates that the R451C mutation does not alter uncaging currents. **(C)** Representative average traces of uEPSCs elicited by MNI-glutamate photorelease at a specific synapse before and 15 min after the delivery of the NMDA protocol. **(D)** Quantification of the fold change of uEPSCs amplitude after the application of the NMDA in WT and KI cultures. The reduction of uEPSC amplitude in WT neurons indicates the expression of LTD. (**G**) Representative averaged uIPSC elicited by DPNI-GABA uncaging at a single inhibitory synapses before and after NMDA application. (**H**) Relative changes of uIPSCs amplitude upon NMDA treatment in WT and KI, as compared to the basal conditions. The increase represents the expression of iLTP (in Wt neurons) whereas the decrease indicates iLTD in KI neurons. Values are expressed as mean ± SEM.*p < 0.05, **p < 0.01, ***p < 0.001, ns = not significant.

Collectively, the results so far indicate that NLGN3 KI neurons fail to express synaptic plasticity in response to NMDA-based stimulation, except for the reverted plasticity observed with uIPSCs (iLTD instead of the iLTP recorded in NLGN3 WT neurons).

8. Larger surface expression of GluN2B in NLGN3 R451C mice

We next evaluated the possibility that changes in the NMDA receptor subunits composition could account for the impaired synaptic plasticity in NLGN3 KI mice. We performed immunocitochemistry assays to probe GluN1, GluN2A and GluN2B subunits of the NMDA receptors at excitatory postsynaptic densities identified by concomitant immunolabeling of PSD-95 (Figure 8A-8C-8E). Quantification of the immunoreactivity of surface GluN1 subunit, on EGFP transfected neurons, indicates that the total expression of this subunit is comparable in NLGN3 WT and NLGN3 KI cells (n=29 and n=12 respectively, p=0.623, t-test, Figure 8B). The total surface expression of GluN2A subunit and its accumulation at excitatory synaptic sites were also comparable in the two genotypes (WT: n= 53 and KI: n=50, total surface expression: p=0.644, t-test, synaptic clusters: p=0.663, t-test; Figure 8D). On the contrary, we quantified that GluN2B subunits were more abundant in NLGN3 KI neurons, as indicated by the larger immunoreactivity detected at the neuronal surface and at synaptic sites, as compared to NLGN3 WT (WT: n=60 and KI: n=55, total surface expression p=0.002, synaptic clusters: p=0.004; Figure 8F). Since it has been previously shown that, with respect to GluN1/N2A, GluN1/N2B heterodimers of NMDA receptors mediate currents with longer decay kinetics (Monyer et al., 1994) and carry more Ca^{2+} per unit of current (Sobczyk et al., 2005), we speculated that the upregulation of such subunit might mediate a higher calcium entry in NLGN3 KI neurons thus interfering with GABAergic plasticity. This hypothesis will be studied in future experiments.

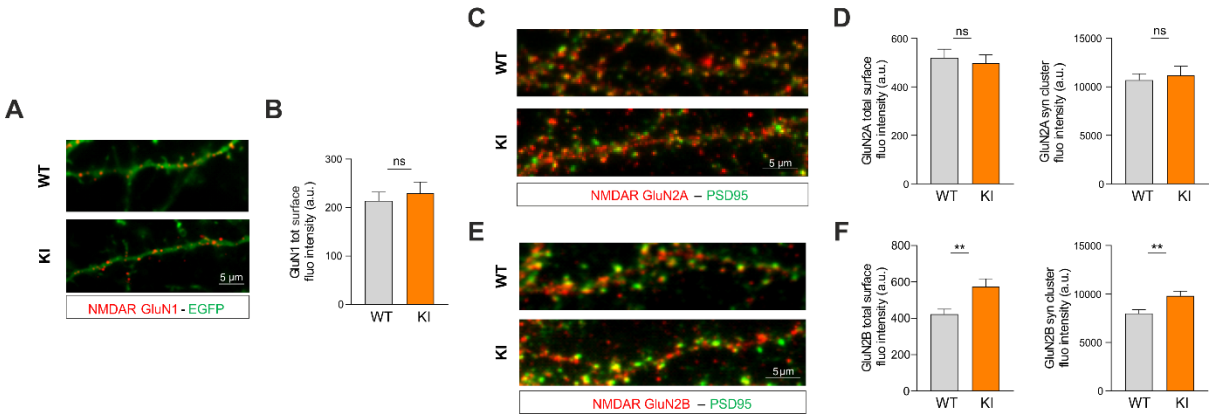

Figure 8. Characterization of NMDA receptor expression in NLGN3 WT and KI neurons. (A) Immunolabeling of surface GluN1 (red) in EGFP-transfected neurons (green) in hippocampal dendrites from WT and NLGN3 KI neurons. Scale bar, 5 µm. **(B)** Quantification of total surface GluN1 average fluorescence intensity detected in NLGN3 WT and KI mice. Please note comparable levels of surface GluN1 in the two genotypes. **(C, E)** Representative images of surface immunolabeling of GluN2A (C) ora GluN2B (E) (red) along with PSD95 (green) in hippocampal dendrites from WT (upper panel) and NLGN3 KI neurons (lower panel). Scale bar, 5 µm. The colocalization of GluN2A or GluN2B fluorescence signal with PSD95 was used to classify clusters as "synaptic". **(D, F)** Quantification of GluN2A (D) and GluN2B (F) immunoreactivity observed at the neuronal surface (left) and in synaptic clusters (right). Please, note the enhanced expression of GluN2B in NLGN3 KI neurons as compared to WT. Values are expressed as mean ± SEM. **p < 0.01, ns = not significant.

DISCUSSION

In the present thesis, by exploiting different approaches, we characterize the properties of excitatory and inhibitory transmission and synaptic plasticity in the NLGN3 R451C KI mouse model of autism. We first, confirmed that NLGN3 KI hippocampal cultures, as previously shown (Tabuchi et al., 2007), exhibit a massive reduction of NLGN3 protein as compared to WT neurons. We then investigated the impact of such NLGN3 reduction at both glutamatergic and GABAergic synapse. In a first round of experiments, we studied the effect of NLGN3 loss in basal conditions and observed that the excitatory and inhibitory synaptic currents (sEPSCs and sIPSCs) were similar in neurons from both wild type and NLGN3 KI mice. In contrast, single particle tracking data revealed that synaptic NLGN3 as well as synaptic α1 and α2 subunit of GABAA receptors were more mobile in NLGN3 KI with respect to wild type. These data reveal that in spite of an overall destabilization of inhibitory synapse organization in NLGN3 KI mice, in basal condition, NLGN3 KI synapses do not show major functional impairments. Such destabilization could be due to either the lack of NLGN3 protein at inhibitory synapses and/or by the defective interaction of NLGN3 R451C with other synaptic proteins. Indeed, in the light of the high degree of cooperation shown by different inhibitory synaptic players (including GABAA receptors), even slight changes in NLGN3 interaction and composition is expected to significantly impact on the dynamic stability of the postsynaptic inhibitory element. Future work addressing the organization of inhibitory synapses in NLGN3 KI mice should focus on the synaptic expression and diffusion properties of key molecular players including e.g. neuroligin 2, collybistin, GARLH4, dystrophin, spectrin, and the different subunits of GABAA receptors, likewise, it will be important to address the important issue of GABAergic diversity. Indeed there are at least 22 interneuronal subclasses form GABAergic synapses on pyramidal neurons that might show substantial differences in function and/or molecular organization. Thus, specific synaptic subsets could be differently affected by the NLGN3 R451C mutation thus influencing specific neuronal circuits. In addition, the fact that the molecular identity of GABAergic synapses may vary among different brain area could further add complexity to the overall effect of the NLGN3 R451C mutation and could provide the molecular basis for the substantial region-specificity of excitatory and inhibitory synaptic currents changes observed in NLGN3 KI mice in previous studies.

Having established that basal excitatory and inhibitory synaptic transmission is similar in wild type and NLGN3 KI mice we next investigated whether the R451C mutation on NLGN3 could

affect the plasticity of glutamatergic and GABAergic synapses. To this end, we adopted a chemical protocol based on a brief NMDA application. This protocol seemed particularly suitable for studying an "integrated" effect of synaptic plasticity on excitation and inhibition since it has been shown to induce long-term depression at glutamatergic synapses and long-term potentiation at GABAergic synapses, respectively (Marsden et al., 2007; Petrini et al., 2014). Interestingly, we found that, the excitatory and inhibitory synaptic plasticity we observed in wild type mice, was absent in the NLGN3 KI genotype since NMDA left sEPSCs and sIPSCs unchanged in mutant mice. In addition, we exploited the uncaging technique that photoreleases neurotransmitter at synapses approaching the synaptic-like conditions to assess the amplitude of uncaging currents before and after the NMDA protocol. We observed that, while in wild type mice uEPSCs were depressed and uIPSCs potentiated, in NLGN3 KI mice, NMDA was unable to induce uEPSCs plasticity and even led to uIPSCs depression. The reverted sign of GABAergic plasticity in KI mice after the NMDA protocol in NLGN3 KI neurons was not observed in spontaneous currents but with the uncaging technique. The nature of this discrepancy might rely on the fact that the spatio-temporal dynamics of GABA following laser uncaging only partially recapitulate that of the physiological GABA release. In particular, in GABA uncaging conditions, we might experience e.g. unwanted activation of extrasynaptic receptors and/or different GABA concentration transient that may in turn change the degree of saturation of synaptic GABAA receptor or may activate different subpopulations of synaptic (and extrasynaptic) GABAA receptors. In summary, the different profile of GABA in the cleft with the uncaging technique might unmask differences not detected in the more physiological context of sIPSCs. Further experiments will be needed to address this issue.

Interestingly, these electrophysiology data were matched by immunocytochemistry experiments. In wild type neurons, after the stimulation, glutamatergic synapses showed reduced expression of GluA1 and GluA2 subunit of AMPA receptor, a well characterized molecular mechanism that has been previously described for NMDA-induced LTD (Genoux et al., 2007). Similarly, we showed an increase of the synaptic levels of α1 and α2 subunit of GABAARs and gephyrin in WT mice. The specificity of mAB7a antibody for phosphorylated gephyrin (Kuhse et al., 2012) might raise the possibility that the higher immunoreactivity of synaptic gephyrin after NMDA treatment might reflect an increase in gephyrin phosphorylation, rather than its accumulation at synapses. However, our data are consistent with previous study from our lab (Petrini et al., 2014) in which we showed that synaptic

gephyrin increase is observed during chem-iLTP by immunocytochemistry also with an alternative anti-gephyrin antibody (mAb3B11).

The molecular mechanisms determining impaired plasticity in NLGN3 KI mice remain to be fully elucidated. It has been clearly shown that at glutamatergic synapses, specific ranges of intracellular calcium concentrations induce different plasticity – low calcium entry attained with low frequency stimulations leads to LTD, while massive calcium entry elicited by stronger stimulations (theta stimulations, high frequency stimulations) induces LTP (Lisman and Zhabotinsky, 2001). Interestingly, previous work demonstrated that, at inhibitory synapses, this calcium rule could be opposite, since mild calcium entry (such as the chemical protocol used here) induced iLTP (Marsden et al., 2007; Petrini et al., 2014; Wiera et al., 2021) while strong calcium entry would rather lead to synaptic depression (Bannai et al., 2009; Muir et al., 2010; Niwa et al., 2012). Such opposite relation between inhibitory and excitatory plasticity suggests a coordinated regulation of shared pathways of signal transduction promoting synaptic plasticity. Indeed, previous study from our lab highlights the involvement of CaMKII activity in iLTP expression (Petrini et al., 2014). In particular, gephyrin recruitment at synapses, is essential for iLTP, but is dependent on CaMKII phosphorylation of the S383 residue of GABAAR ß3 subunit. In this way, GABAAR are accumulated and retained at synapses mediating increased inhibitory synaptic responses. So, CaMKII plays a crucial role in downstream cascade signal regulating both excitatory and inhibitory transmission. It is able to translocate to glutamatergic postsynaptic density after strong activity promoting LTP at glutamatergic synapses (Shen and Meyer, 1999; Merrill et al., 2005) while weaker stimuli resulting in lower calcium entry localize CaMKII at inhibitory synapses where it endows iLTP (Marsden et al., 2010). In this scenario, one possibility is that in NLGN3 KI neurons, the calcium variation induced by NMDA stimulation is oustide the “calcium window” for the correct expression of LTD and iLTP in NLGN3 WT neurons. Such alteration of calcium dynamics in NLGN3 R451C KI mice could be due to the enhanced incorporation of the GluN2B subunit, which might concur in impairing excitatory and inhibitory plasticity since this subunit might mediate a higher NMDA receptors conductance (Bellone and Nicoll, 2007). At this stage, however, we cannot distinguish between the possibilities that calcium concentration dynamics in NLGN3 KI neurons would be i) insufficient to induce correct plasticity or ii) exaggerated thus leading to the “saturation” of the plasticity machinery. Further experiments exploring the plasticity in response to induction protocols of different intensities and duration could in principle address this point.

Interestingly, in NLGN3 KI mice, we observed a higher expression of α2 GABAA receptors subunit compared to wild type. α2-containing receptors are known to mediate anxiolytic-like, reward-enhancing, and antihyperalgesic actions of diazepam, and show antidepressant-like properties (Engine et al., 2012). Accordingly, recent evidence suggests that the anxiolytic effect of benzodiazepines (BZs) is mediated by the GABAAR α2 subunit and elevated numbers of α2-containing GABAARs may potentially enhance the GABAAR response to anxiety and stress (Low et al., 2000). Neonatal handling and brief maternal separation have been shown to lead to an increase in the expression of the α2 subunit in the dentate gyrus of adult animals, and to increased activity in response to swim stress (Hsu, et al., 2003). Thus, stress in NLGN3 KI mice during development might induce changes in the expression pattern of GABAA receptor subtypes. In these conditions, the increase of the α2 subunit expression could be interpreted as a compensatory mechanism that, although insufficiently, is aimed at coping with the negative effects of the NLGN3 R451C mutation.

We found that, following NMDA stimulation, NLGN3 protein expression decreases at inhibitory synapses of wild type mice along with its increased immobilization. While the mechanism of such effect remains unaddressed in the present study, it could be hypothesized that NLGN3 could undergo cleavage. Matrix metalloproteases (MMPs), for example, are a Zn^{2+}-large family of secreted dependent proteolytic enzymes that cleave extracellular matrix components and pericellular proteins (Ethell and Ethell, 2007; Yong, 2005). It has been demonstrated that MMP9 is acutely upregulated and secreted in response to neuronal activity and is required for the expression of LTP (Bozdagi et al., 2007; Nagy et al., 2006; Wang et al., 2008). Interestingly, MMP9-mediated cleavage of NLGN1 is known to occur throughout development, and is upregulated by neuronal activity in mature and developing circuits (Peixoto et al., 2012). Moreover, some CAMs such as N-Cadherin, ICAM-5, NCAM, and L1-CAM can be cleaved during the induction of LTP, and disruptions to the function of these CAMs can result in impaired plasticity (Lüthl et al., 1994; Fazeli et al., 1994; Reiss et al., 2005; Conant et al., 2010; Niedringhaus et al., 2012). Therefore, even if, to our knowledge, activity-dependent cleavage of NLGN3 has not been shown so far, it could explain the downregulation of NLGN3 surface protein in WT neurons after the NMDA application. In line with an activity dependent mechanism, in the case of reduced synaptic NLGN3 protein, the presynaptic NLGN3 binding site (e.g. neurexins) could outnumber the remaining NLGN3 thus explaining the increased NLGN3 immobility at synapses. Alternatively, fast internalization of NLGN3 or e.g. calcium mediated activity dependent NLGN3 immobilization could also explain the

NLGN3 effects during plasticity. In contrast to wild type, in NLGN3 KI mice, NLGN3 showed similar expression and mobility before and after the NMDA treatment. We speculate that either the lack of NLGN3 or the presence of defective NLGN3 R451C alter in NLGN3 KI mice the molecular rearrangements and interactions occurring in wild type mice during NMDA plasticity expression.

The results on excitatory and inhibitory synaptic plasticity shown in the present study are in line with a perturbation of E/I balance, which is a common feature in different mice model of ASD. However, the impact of such altered plasticity on excitation-to-inhibition ratio at the level of specific circuits and microcircuits is unknown. Indeed, different circuits may be characterized by specific levels of excitation and inhibition and, even within a single neuron, changes of the E/I in neuronal sub-domains (soma, proximal and distal dendrites) could interfere with network activity of NLGN3 R451C KI mice. Future experiments will ne needed to tackle this issue in ex vivo and in vivo to test whether the plasticity alterations observed in KI cultured neurons similarly e.g. affect different interneuron subtypes which are known to contact different region of the pyramidal cells. Perisomatic inhibition, mainly mediated by PV^+ interneurons, largely regulates neuronal spike output and exhibits forms of plasticity coupled to postsynaptic action potentials while dendritic inhibition, mediated by SOM^+ interneurons, regulates local electrical and biochemical signalling and can undergo plasticity coupled to excitatory glutamatergic activity (Chiu et al., 2019). Therefore, different players in setting a dynamic balance between excitation and inhibition may coexist at the single neuron level. Our laboratory is currently exploring these possibilities, by characterizing inhibitory plasticity in these specific GABAergic microcircuits involved in feedback and feedforward inhibition.

Overall, our data reinforce the hypothesis that alterations of synaptic plasticity represent a convergent mechanism underlying several neuro-developmental disorders including ASD (Baudouin et al., 2012). By studying the coordinated plasticity at both excitatory and inhibitory synapses, we have found that, in an animal model of ASD, excitatory and inhibitory synapses are unable to tune their strength in response to plasticity-inducing protocols. This could be an important determinant of network malfunctioning and aberrant signal processing.

The present data could inspire future work aimed at ascertain the molecular players involved in the induction and expression of defective synaptic plasticity to restore the correct activity-dependent changes of excitatory and inhibitory synapses. This will lead to the identification of

novel molecular targets in ASD that might eventually lead to the creation of new therapeutic avenues.

EXPERIMENTAL PROCEDURES

1. Animals

All experiments were carried out in accordance with the guidelines established by the European Communities Council (Directive 2010/63/EU of 22 September 2010), were approved by the Italian Ministry of Health and followed the rules of the Italian Institute of Technology concerning experimentation with animals. The experiments were conducted on the NLGN3 R451C KI (B6;129-*Nlgn3*^{tm1Sud}/J) mouse strain (Jackson Laboratories, Maine, USA, Jax stock #008475) which is considered a model of ASD (Etherton et al., 2011a; Tabuchi et al., 2007) and on their wild-type counterparts.

In NLGN3 KI transgenic mice the cell adhesion protein NLGN3 carries the R451C mutation in exon 7 of the *Nlgn3* gene. Exon 7 is flanked by loxP sites. Since the *Nlgn3* gene is located on the X chromosome, mice breeding could deliver homozygous (F NLGN3-KI+/+), heterozygous (F NLGN3-KI+/-) or hemizygous (M NLGN3-KI+/Y) mice. Homozygous and hemizygous mice for the target mutation are viable, fertile, of normal size, and show no major physical abnormalities.

NLGN3 WT mice derived from the NLGN3-KI transgenic strain. We initially crossed heterozygous F (NLGN3-KI+/-) x hemizygous M (NLGN3-KI+/Y) to obtain wild-type M (NLGN3-WT) and subsequently, we crossed heterozygous F (NL3-KI+/-) with the aforementioned wild-type M. Thus, this NLGN3-WT colony has exon 7 of the *Nlgn3* gene flanked by loxP sites. They are viable and fertile mice with no phenotype alterations.

2. Cell culture and transfection

Primary cultures of hippocampal neurons were prepared from NLGN3 WT and NLGN3 R451C KI mouse pups (P1-3). Briefly, hippocampi were dissected, quickly sliced and digested with trypsin in the presence of DNAase, mechanically triturated, centrifuged at 80g and re-suspended. Neurons were plated at a density of 90000 cells on 18-mm diameter glass coverslips, coated with 0.1 % poly-L-lysine (Sigma-Aldrich). Cells were kept in a maintenance medium composed of Neurobasal A medium (GIBCO, Invitrogen, Germany) supplemented with B27 (1X), L-glutamine (2 mM), and Gentamycin 0.5% (Invitrogen) up to 3 weeks at 37°C

in a 5% CO2 humidified incubator. At day in vitro (DIV) 7, new maintenance medium was added to the old one (1:5). Neurons were transfected with DNA plasmids either using Effectene (Qiagen, Germany) at 6-7 days in vitro (DIV) or Lipofectamine 2000 (Thermofisher) 24/72 hours before the experiments, following the companies' protocols. These plasmids included EGFP, Homer1c-DsRed, Homer1c-EGFP, NLGN3 WT-HA, $NLGN3^{R451C}$ –HA, gephyrin-EGFP. Enhanced GFP (eGFP) was expressed from the pEGFP-N1 (Clontech). Homer1c-DsRed plasmid encoding for Homer1c fused with DsRed or EGFP at the N terminus, were kindly provided by Dr. D. Choquet (Petrini et al., 2009). NLGN3 WT-HA and EGFP-gephyrin were a gift from Prof. E. Cherubini. $NLGN3^{R451C}$ -HA was obtained by site directed mutagenesis (QuickChange II Site-Directed Mutagenesis Kit, Agilent Technologies) of R451 residue and confirmed by DNA sequencing. All experiments were performed between 14 DIV and 21 DIV.

3. NMDA treatment

NMDA treatment was used as a chemical approach to induce synaptic plasticity as previously described (Marsden 2007, Petrini 2014). Hippocampal cells were stimulated with a recording solution (145mM NaCl, 5mM KCl, 10mM HEPES, 1mM CaCl2, 2mM MgCl2, 10Mm D-serine, 5.5mM glucose; pH 7.4; ~300mOsm) supplemented with NMDA (20μM) and CNQX (10μM) for 2 min at 37°C and then allowed a recovery period of 20 minutes in bare recording solution. In case of live experiments (electrophysiology and single particle tracking recordings), recordings were performed during the recovery period up to 30 min, if possible. In the case of immunocytochemistry experiments, samples were fixed after 20 min recovery.

4. Immunocitochemistry

In immunocytochemistry experiments, neurons were fixed for 10 min in 4% paraformaldehyde (PFA) and then incubated for 10 minutes in a blocking solution (BSA 1%) to prevent aspecific antibody binding. Next, neurons were incubated for 1 hour with a primary antibody to reveal surface proteins and subsequently with appropriate specie-specific secondary fluorescent antibodies for 45 min. In particular, we used the following primary antibodies recognizing: GABAAR α1 subunit (1:100, Alomone Labs, Israel); GABAAR α2 subunit (1:500, Synaptic

Systems, Germany); GluA1 (1:400, Neuromab); GluA2 (1:200, Millipore); GluN1 (1:100, Alomone Labs, Israel); GluN2A (1:100, Alomone Labs, Israel); GluN2B (1:1000, Alomone Labs, Israel); PSD-95 (1:500, Euroclone); gephyrin (mAB7a, 1:150, Synaptic System, Germany), HA (1:1000, rat, Roche, Swiss) and the secondary antibodies coupled to Alexa 488, 568 or 647 (1:500; Molecular Probes, Invitrogen, Italy). Immunostainings of intracellular proteins such as Homer, PSD-95 and vGAT were performed after permeabilization (0.2% Triton X-100 for 10 min) and sequential incubation with primary antibodies as indicated above and appropriate secondary antibodies. All coverslips were mounted in DAKO fluorescence mounting medium and kept at 4°C.

5. Fluorescence image acquisition and analysis

Acquisition and quantification were performed using MetaMorph 7.7 (Molecular Devices). Images were acquired with a digital camera (Hamamatsu, EM-CCD C9100) mounted on a wide field inverted fluorescence microscope (Nikon Eclipse Ti) equipped with an oil immersion 60X objective (1.4 NA) or 100X. Samples were illuminated with a LED light source (Spectra X, Lumencor) through 475/34 nm, 543/22 and 628/40 filters (Semrock, Italy) to excite for Alexa488, Alexa568 and Alexa647 fluorescence. The same exposure time was applied to all samples and was set in order to avoid signal saturation. The total average fluorescence intensity of a protein was calculated as the integrated fluorescence intensity detected on the dendritic surface, divided by its area, and expressed as “total surface intensity”. After fast fourier transform (FFT), a user-defined intensity threshold was applied to each image to identify clusters and avoid their coalescence. The clusters were considered synaptic when their position colocalized with or was juxtaposed to (within 2 pixels) the postsynaptic or presynaptic fluorescence signal, respectively. Background fluorescence was subtracted from all images before analysis. Quantification included clusters of at least 3 pixels.

6. Quantum Dot labeling and synapse labeling

The experiments aimed at assessing the lateral mobility of NLGN3 were performed in cultured hippocampal neurons from NLGN3 WT and KI mice transfected with HA-tagged NLGN3-WT or -KI, respectively. Excitatory synapses were localized by co-transfection with Homer-GFP.

Inhibitory synapses were identified by live immunolabeling of the presynaptic protein vGAT using the specific anti-vGAT-Oyster550 antibody (Synaptic Systems, Germany) which is directed towards the domain exposed to the luminal side of the released synaptic vesicle, diluted in culture medium and incubated for 30 min at 37°C.

In SPT experiments, the protein of interest are tracked by applying a specific antibody (directed towards an extracellular epitope) coupled to quantum dots (QDs). QDs are nanometer sized semiconductors which emit fluorescence due to a core fluorescent moiety of CdSe surrounded by a ZnS shell and covered with an organic shell meant to enhance QD biocompatibility. The QD fluorescence shows strong photostability with moderate photobleaching over long illumination periods and high signal /noise ratio. These peculiarities allow stable recordings of the diffusion of the receptor-QD complex with ~ 40 nm accuracy (Bannai et al., 2006). Before the experiment, QDs 655 (Invitrogen) were diluted in PBS and pre-exposed to casein 1X (Vectorlab, Italy) for 15 min to prevent QD aspecific binding. Then, living neurons were incubated with the appropriate antibody (anti-HA, anti-α1 or anti- α2, see above) at a 1 mg/mL concentration in the recording solution for 3 minutes and subsequently with the diluted QDs solution for 3 minutes in order to allow sparse labeling. The final concentration of QD was 0.1 nM. Control experiments omitting the primary antibody were performed to validate the antibody-specific labelling. The strong dilution of QDs with respect to the antibody concentration likely allows tracking of individual receptors. All washes were performed in recording solution.

7. Single Particle Imaging and Tracking

Cultured neurons were imaged at 32°C (TC-324B Warner Instrument Corporation, CT, USA) in an open chamber continuously perfused with the recording solution (see above) at 12 ml/h, mounted onto a wide field inverted fluorescence microscope (Nikon Eclipse Ti). Samples were illuminated with a diode-based illumination device (Lumencor, SpectraX Light Engine, Optoprim, Italy) and observed with an oil immersion 60X objective (1.4 NA) or 100x (1.4 NA).

QD fluorescence was acquired with specific filters (ex: 435/40 and em: 655/15 filters, Semrock, Italy) over time by recording movies of 1200 consecutive frames at 20 Hz using the Metamorph 7.8 software (Molecular Devices, USA) to control an EM-CCD camera (8 Hamamatsu, EM-CCD C9100). When the NMDA stimulation was applied in the SPT experiments, the mobility

of QD was probed in the same field of view before and up to 30 minutes after the induction of synaptic plasticity. Two consecutive one-min long movies were recorded at each time point to take into account the variability in the diffusive behavior of surface receptors.

For the single QD tracking, trajectories were reconstructed using Metamorph 7.7 and home written software (kindly provided by Dr. Choquet and subsequently implemented in our laboratory) developed in MatLab (The Mathworks Inc., Italy). The spatial coordinates of single QDs were identified in each frame as sets of >4 connected pixels using two-dimensional object wavelet-based localization, at sub-diffraction limited resolution (40 nm) using the MIA software (Racine et al. 2007) which is based on simulated annealing algorithm. Continuous tracking between blinks was performed with a method based on a QD maximal allowable displacement (4 pixels) during a maximal allowable duration of the dark period (25 frames, corresponding to 1.25 s acquisition). Subtrajectories of single QDs with > 100 points were retained for analysis and were defined as 'synaptic' when their spatial coordinates coincided with those of the postsynaptic compartment or were included within a 2 pixel enlargement of the presynaptic marker. Trajectories, reconstructed at synaptic and extrasynaptic sites, were used to measure the receptor diffusion coefficient at each compartment. Instantaneous diffusion coefficients, D, were calculated as previously described (Tardin et al., 2003) by fitting the first 4 points of the mean squared displacement (MSD) versus time curves with the equation: $MSD(n\tau)=4Dn\tau$ describing 2D free diffusion. MSD(t) was calculated according to the formula:

$$<r^2> = [\Sigma_{i=1}^{(N-n)} (X_{i+n} - X_i)^2 + (Y_{i+n} - Y_i)^2 / (N-n)]dt$$

D is expressed as median ± IQR, defined as the interval between 25–75% percentile. The immobile fraction is defined as the relative duration of the residency of a QD in a given compartment with coefficient < 0.0075 $\mu m^2 s^{-1}$, which is the local minimum of the bimodal distribution of D values.

8. Electrophysiological recordings

Spontaneous inhibitory and excitatory postsynaptic currents (sIPSCs and sEPSCs, respectively) were recorded at room temperature in the whole-cell configuration of the patch-clamp technique. External recording solution contained (in mM): 145mM NaCl, 5mM KCl, 10mM HEPES, 1mM CaCl2, 2mM MgCl2, 10mM D-serine, 5.5mM glucose; pH 7.4;

~300mOsm. Patch pipettes, pulled from borosilicate glass capillaries (Warner Instruments, LLC, Hamden, USA) had a 4 to 5 MΩ resistance when filled with intracellular solution. In all experiments the intracellular solution contained (in mM): 10 KGluconate, 125 KCl, 1 EGTA, 10 HEPES, 5 Sucrose, 4 MgATP (300mOsm and pH 7.2 with KOH). sIPSCs and sIPSCs were recorded at room temperature from a holding potential of −65 mV. sIPSC were recorded in the presence of CNQX (10 μM) to isolate GABAergic events. NMDAR activation was used to induce iLTP and LTD as previously described. The electrophysiology data in each experiment were obtained by recording sIPSCs and sEPSC from the same neuron before and after NMDA treatment up to 30 min.

In each experiment, the stability of the patch was checked by repeatedly monitoring the input resistance to exclude cells exhibiting more than 15% changes from the analysis. Currents were sampled at 20 KHz and digitally filtered at 3 KHz using the 700B Axopatch amplifier (Molecular Devices, Sunnyvale, CA). IPSCs and EPSCs were analyzed with Clampfit 10.0 (Molecular Devices, Sunnyvale, CA). sIPSCs and sEPSCs were detected by using the 'scaled sliding template' detection algorithm implemented in pClamp10, first described by Clements and Bekkers and by setting the 'detection criterion value' to 5.

9. Neurotransmitter uncaging

GABA and Glutamate were photoreleased from DPNI-GABA and MNI-glutamate after illumination by a 378 nm diode laser (Cube 378, 16 mW, Coherent Italia, Italy). MNI-glutamate (5 mM) or DPNI-GABA (1 mM) were dissolved in extracellular solution and locally applied near the synapses through a pulled glass capillary (2-4 μm tip diameter) placed at 10-30 μm in the x-axis and at 5-10 μm in the z-axis from the region of interest (ROI), using a pressure-based perfusion system (5/10 psi) (Picospritzer, Parker, USA). The laser beam was focused on the sample by means of an Olympus Apo-plan 100X oil-immersion objective (1.4 NA). A beam expander was placed in the optical path between the laser source and the objective in order to achieve a complete filling of the objective pupil, a condition that maximizes the focusing capability of the objective, thus minimizing the spot size on the sample. The measured point spread function (PSF) had a lateral dimension of 487±55 nm (FWHM, n = 6). The laser beam was steered in the field of view by using a galvanometric mirrors-based pointing system able to illuminate specific regions of interest outlined around glutamatergic and GABAergic

synapses defined by Homer1c-DsRed and gephyrin-EGFP (UGA32, Rapp OptoElectronics, Hamburg, Germany). Synchronization of optical uncaging and electrophysiological recordings was controlled with the UGA32 software interfaced with the Clampex 10.0 software (Molecular Devices, Sunnyvale, CA, USA). Both MNI-glutamate and DPNI-GABA uncaging currents (uEPSCs and uIPSCs, respectively) were elicited by 500-1000 µs laser pulses with a power intensity of 80-100 µW at the exit of the objective. The uncaged excitatory and inhibitory currents were recorded before and 15 minutes after the NMDA-inducing plasticity protocol.

10. Statistics

For each experiment quantifications and statistical details (statistical significance and test used) can be found in the main text and figure legends. Unless otherwise stated, normally distributed data are presented as mean ± SEM (standard error of the mean), whereas non-normally distributed data are given as medians ± IQR (inter quartile range). Normally distributed data sets were compared using the two-tailed Student's t-test (paired in some instances), whereas non-Gaussian data sets were tested by two-tailed non-parametric Mann–Whitney U-test or Wilcoxon matched pairs test. Statistical differences in time course data within a group (e.g. expression of synaptic plasticity) was assessed by one-way ANOVA variance test followed by Tukey's multiple comparison test. When possible, RM ANOVA was used, as indicated .Two-way ANOVA test was used to analyze the Mean square displacement in Single particle tracking experiments. For SPT experiments, n indicates the number of receptor trajectories. In immunocytochemistry and electrophysiology experiments n indicates the number of cells analysed. Each type of experiment was repeated on neurons obtained from at least three different cultures. Indications of significance correspond to P-values < 0.05 (*), P<0.01 (**), P<0.001 (***) and nonsignificant (ns).

REFERENCES

Akins, M. R., & Biederer, T. (2006). Cell-cell interactions in synaptogenesis. Current Opinion in Neurobiology, 16(1), 83–9. doi:10.1016/j.conb.2006.01.009

Antoine MW, Langberg T, Schnepel P, Feldman DE. Increased Excitation-Inhibition Ratio Stabilizes Synapse and Circuit Excitability in Four Autism Mouse Models. Neuron. 2019 Feb 20;101(4):648-661.e4

Arac, D., Boucard, A. A., Ozkan, E., Strop, P., Newell, E., Sudhof, T. C., et al. (2007). Structures of neuroligin-1 and the neuroligin-1/neurexin-1 beta complex reveal specific protein-protein and protein-Ca2+ interactions. Neuron 56, 992–1003

Bacchelli, E., & Maestrini, E. (2006). Autism spectrum disorders: Molecular genetic advances. American Journal of Medical Genetics. Part C, Seminars in Medical Genetics, 142C(1), 13–23

Baig, D.N., Yanagawa, T., Tabuchi, K., 2017. Distortion of the normal function of synaptic cell adhesion molecules by genetic variants as a risk for autism spectrum disorders. Brain Res. Bull. 129, 82–90

Baio, J., Wiggins, L., Christensen, D. L., Maenner, M. J., Daniels, J., Warren, Z., et al. (2018). Prevalence of autism spectrum disorder among children aged 8 years - Autism and developmental disabilities monitoring network, 11 sites, United States, 2014. MMWR Surveillance Summaries, 67(6), 1–23

Bannai, H., Lévi, S., Schweizer, C., Inoue, T., Launey, T., Racine, V., Sibarita, J.B., Mikoshiba, K., and Triller, A. (2009). Activity-Dependent Tuning of Inhibitory Neurotransmission Based on GABAAR Diffusion Dynamics. Neuron 62, 670–682

Bariselli, S., Hornberg, H., Prevost-Solie, C., Musardo, S., Hatstatt-Burkle, L., Scheiffele, P., et al. (2018). Role of VTA dopamine neurons and neuroligin 3 in sociability traits related to nonfamiliar conspecific interaction. Nat. Commun. 9:3173

Barnard, E. A., Skolnick, P., Olsen, R. W., Mohler, H., Sieghart, W., Biggio, G., et al. (1998). International Union of Pharmacology. XV. Subtypes of gammaaminobutyric acid A receptors: classification on the basis of subunit structure and receptor function. Pharmacol. Rev. 50, 291–313

Baudouin, S. J., Gaudias, J., Gerharz, S., Hatstatt, L., Zhou, K., Punnakkal, P., et al. (2012). Shared synaptic pathophysiology in syndromic and nonsyndromic rodent models of autism. Science 338, 128–132

Bellone C, Nicoll RA. Rapid bidirectional switching of synaptic NMDA receptors. Neuron. 2007 Sep 6;55(5):779-85

Bemben, M. A., Nguyen, T. A., Li, Y., Wang, T., Nicoll, R. A., and Roche, K. W. (2019). Isoform-specific cleavage of neuroligin-3 reduces synapse strength. Mol. Psychiatry 24, 145–160

Biederer T, Südhof TC. CASK and protein 4.1 support F-actin nucleation on neurexins. J Biol Chem 2001;276:47869–47876

Blasi, F., Bacchelli, E., Pesaresi, G., Carone, S., Bailey, A. J., Maestrini, E., et al. (2006). Absence of coding mutations in the X-linked genes neuroligin 3 and neuroligin 4 in

individuals with autism from the IMGSAC collection. Am. J. Med. Genet. B Neuropsychiatr. Genet. 141B, 220–221

Bliss TVP, Lømo T. Long-lasting potentiation of synaptic transmission in the dentate area of the anaesthetized rabbit following stimulation of the perforant path. J. Physiol. 1973; 232: 331–56

Boddaert N Zilbovicius M Philipe A et al. . MRI findings in 77 children with non-syndromic autistic disorder. PLoS One,2009;4:e4415

Bölte, S., Girdler, S., & Marschik, P. B. (2018). The contribution of environmental exposure to the etiology of autism spectrum disorder. Cellular and Molecular Life Sciences, 76(7), 1275–1297

Bolton PF, Carcani-Rathwell I, Hutton J, Goode S, Howlin P, Rutter M. Epilepsy in autism: features and correlates. Br J Psychiatry. 2011 Apr;198(4):289-94

Boucard A, Chubykin AA, Comoletti D, Taylor P, Südhof TC. A splice-code for trans-synaptic cell adhesion mediated by binding of Neuroligin 1 to α- and β-Neurexins. Neuron 2005;48:229–236

Bozdagi, O., Nagy, V., Kwei, K. T., & Huntley, G. W. (2007). In vivo roles for matrix metalloproteinase-9 in mature hippocampal synaptic physiology and plasticity. Journal of Neurophysiology, 98(1), 334–44

Bozzi Y, Provenzano G, Casarosa S. Neurobiological bases of autism-epilepsy comorbidity: a focus on excitation/inhibition imbalance. Eur J Neurosci. 2018;47(6):534–48

Budreck, E. C., & Scheiffele, P. (2007). Neuroligin-3 is a neuronal adhesion protein at GABAergic and glutamatergic synapses. European Journal of Neuroscience, 26(August), 1738–1748

Burrows, E. L., Eastwood, A. F., May, C., Kolbe, S. C., Hill, T., McLachlan, N. M., et al. (2017). Social Isolation Alters Social and Mating Behavior in the R451C Neuroligin Mouse Model of Autism. Neural Plast. 2017:8361290

Burrows, E. L., Koyama, L., May, C., Hill-Yardin, E. L., and Hannan, A. J. (2020). Environmental enrichment modulates affiliative and aggressive social behaviour in the neuroligin-3 R451C mouse model of autism spectrum disorder. Pharmacol. Biochem. Behav. 195:17295

Burrows, E. L., Laskaris, L., Koyama, L., Churilov, L., Bornstein, J. C., Hill- Yardin, E. L., et al. (2015). A neuroligin-3 mutation implicated in autism causes abnormal aggression and increases repetitive behavior in mice. Mol. Autism 6:62

Cajigas, I. J., Tushev, G., Will, T. J., tom Dieck, S., Fuerst, N., and Schuman, E. M. (2012). The local transcriptome in the synaptic neuropil revealed by deep sequencing and high-resolution imaging. Neuron 74, 453–466

Castillo, P. E., Janz, R., Sudhof, T. C., Tzounopoulos, T., Malenka, R. C., and Nicoll, R. A. (1997). Rab3A is essential for mossy fibre long-term potentiation in the hippocampus. Nature 388, 590–593. doi:10.1038/41574

Castillo, P. E., Schoch, S., Schmitz, F., Südhof, T. C., and Malenka, R. C. (2002). RIM1alpha is required for presynaptic long-term potentiation. Nature 415, 327–330. doi:10.1038/415327a

Castillo, P.E. (2012). Presynaptic LTP and LTD of excitatory and inhibitory synapses. Cold Spring Harb. Perspect. Biol. 4

Castillo, P.E., Chiu, C.Q., and Carroll, R.C. (2011). Long-term plasticity at inhibitory synapses. Curr. Opin. Neurobiol. 21, 328–338

Cellot, G., and Cherubini, E. (2014). Reduced inhibitory gate in the barrel cortex of Neuroligin3R451C knock-in mice, an animal model of autism spectrum disorders. Physiol. Rep. 2:12077

Chadman, K. K., Gong, S., Scattoni, M. L., Boltuck, S. E., Gandhy, S. U., Heintz, N., et al. (2008). Minimal aberrant behavioral phenotypes of neuroligin-3 R451C knockin mice. Autism Res. 1, 147–158

Chao, H.-T., Chen, H., Samaco, R.C., Xue, M., Chahrour, M., Yoo, J., Neul, J.L., Gong, S., Lu, H.-C., Heintz, N., et al. (2010). Dysfunction in GABA signaling mediates autism-like stereotypies and Rett syndrome phenotypes. Nature 468, 263–269

Chevaleyre, V., and Castillo, P.E. (2003). Heterosynaptic LTD of hippocampal GABAergic synapses: a novel role of endocannabinoids in regulating excitability. Neuron 38, 461–472

Chevaleyre, V., Heifets, B. D., Kaeser, P. S., Südhof, T. C., Purpura, D. P., and Castillo, P. E. (2007). Endocannabinoid-Mediated Long-Term Plasticity Requires cAMP/PKA Signaling and RIM1?? Neuron 54, 801–812

Chevaleyre, V., Takahashi, K. A., and Castillo, P. E. (2006). Endocannabinoidmediated synaptic plasticity in the CNS. Annu. Rev. Neurosci. 29, 37–76

Chih B, Gollan L, Scheiffele P. Alternative splicing controls selective trans-synaptic interactions of the neuroligin-neurexin complex. Neuron 2006;51:171–178

Chih, B., Afridi, S. K., Clark, L., and Scheiffele, P. (2004). Disorder-associated mutations lead to functional inactivation of neuroligins. Hum. Mol. Genet. 13, 1471–1477

Chiu, C.Q., Barberis, A., and Higley, M.J. (2019). Preserving the balance: diverse forms of long-term GABAergic synaptic plasticity. Nat. Rev. Neurosci. *20*, 272–281

Chiu, C.Q., Martenson, J.S., Yamazaki, M., Natsume, R., Sakimura, K., Tomita, S., Tavalin, S.J., and Higley, M.J. (2018). Input-Specific NMDAR-Dependent Potentiation of Dendritic GABAergic Inhibition. Neuron 97, 368-377.e3

Chocholska S, Rossier E, Barbi G, Kehrer-Sawatzki H. Molecular cytogenetic analysis of a familial interstitial deletion Xp22.2–22.3 with a highly variable phenotype in female carriers. Am J Med Genet A 2006;140:604–610

Choquet, D., & Triller, A. (2013). The dynamic synapse. Neuron, 80(3), 691–703

Chubykin AA, et al. Activity-dependent validation of excitatory vs. inhibitory synapses by neuroligin-1 vs. neuroligin-2. Neuron 2007;54:919–931

Clements, J. D. & Bekkers, J. M. Detection of spontaneous synaptic events with an optimally scaled template. Biophys. J. 73, 220–229 (1997)

Comoletti D, et al. Gene selection, alternative splicing, and post-translational processing regulate neuroligin selectivity for β-neurexins. Biochemistry 2006;45:12816–12827

Comoletti, D., De Jaco, A., Jennings, L. L., Flynn, R. E., Gaietta, G., Tsigelny, I., et al. (2004). The Arg451Cys-neuroligin-3 mutation associated with autism reveals a defect in protein processing. J. Neurosci. 24, 4889–4893

Conant K, Wang Y, Szklarczyk A, Dudak A, Mattson MP, Lim ST. Matrix metalloproteinase-dependent shedding of intercellular adhesion molecule-5 occurs with long-term potentiation. Neuroscience. 2010;166(2):508–521

Constantino, J. N., Zhang, Y., Frazier, T., Abbacchi, A. M., & Law, P. (2010). Sibling recurrence and the genetic epidemiology of autism. The American Journal of Psychiatry, 167(11), 1349–1356

Cooper, M. W., & Smith, S. J. (1992). A real-time analysis of growth cone-target cell interactions during the formation of stable contacts between hippocampal neurons in culture. Journal of Neurobiology, 23(7), 814–28. doi:10.1002/neu.480230704

Craig, A.M., Kang, Y., 2007. Neurexin-neuroligin signaling in synapse development. Curr. Opin. Neurobiol. 17, 43–52

Dani, V.S., Chang, Q., Maffei, A., Turrigiano, G.G., Jaenisch, R., and Nelson, S.B. (2005). Reduced cortical activity due to a shift in the balance between excitation and inhibition in a mouse model of Rett syndrome. Proc. Natl. Acad. Sci. USA 102, 12560–12565

Davis GW. Homeostatic control of neural activity: from phenomenology to molecular design. Annu Rev Neurosci. 2006; 29:307–323

De Jaco, A., Lin, M. Z., Dubi, N., Comoletti, D., Miller, M. T., Camp, S., et al. (2010). Neuroligin trafficking deficiencies arising from mutations in the alpha/betahydrolase fold protein family. J. Biol. Chem. 285, 28674–28682

De la Torre-Ubieta, L., Won, H., Stein, J. L., and Geschwind, D. H. (2016). Advancing the understanding of autism disease mechanisms through genetics. Nat. Med. 22, 345–361. doi: 10.1038/nm.4071

De Rubeis S et al. (2014) Synaptic, transcriptional and chromatin genes disrupted in autism. Nature 515, 209–215

De Rubeis, S., and Buxbaum, J. D. (2015). Genetics and genomics of autism spectrum disorder: embracing complexity. Hum. Mol. Genet. 24, R24–R31. doi: 10.1093/hmg/ddv273

Dean, C., Scholl, F. G., Choih, J., DeMaria, S., Berger, J., Isacoff, E., et al. (2003). Neurexin mediates the assembly of presynaptic terminals. Nat. Neurosci. 6, 708–716

Delattre, V., La Mendola, D., Meystre, J., Markram, H., and Markram, K. (2013). Nlgn4 knockout induces network hypo-excitability in juvenile mouse somatosensory cortex in vitro. Sci. Rep. 3, 2897

Diana, M. A., and Marty, A. (2004). Endocannabinoid-mediated short-term synaptic plasticity: depolarization-induced suppression of inhibition (DSI) and depolarization-induced suppression of excitation (DSE). Br. J. Pharmacol. 142, 9–19

Dingledine R, Borges K, Bowie D, Traynelis SF. The glutamate receptor ion channels. *Pharmacol. Rev.* 1999; 51: 7π61

Engin E, Liu J, Rudolph U. α2-containing GABA(A) receptors: a target for the development of novel treatment strategies for CNS disorders. Pharmacol Ther. 2012 Nov;136(2):142-52

Engin E, Liu J, Rudolph U. α2-containing GABA(A) receptors: a target for the development of novel treatment strategies for CNS disorders. Pharmacol Ther. 2012 Nov;136(2):142-52

Ethell, I. M., & Ethell, D. W. (2007). Matrix metalloproteinases in brain development and remodeling: synaptic functions and targets. Journal of Neuroscience Research, 85(13), 2813–23

Etherton MR, Blaiss CA, Powell CM, Sudhof TC. 2009. Mouse neurexin-1a deletion causes correlated electrophysiological and behavioral changes consistent with cognitive impairments. Proc Natl Acad Sci 42: 7998–8003

Etherton, M. R., Tabuchi, K., Sharma, M., Ko, J., and Sudhof, T. C. (2011). An autism-associated point mutation in the neuroligin cytoplasmic tail selectively impairs AMPA receptor-mediated synaptic transmission in hippocampus. EMBO J. 30, 2908–2919

Etherton, M., Foldy, C., Sharma, M., Tabuchi, K., Liu, X., Shamloo, M., et al. (2011). Autism-linked neuroligin-3 R451C mutation differentially alters hippocampal and cortical synaptic function. Proc. Natl. Acad. Sci. U S A. 108, 13764–13769

Fazeli MS, Breen K, Errington ML, Bliss TVP. Increase in extracellular NCAM and amyloid precursor protein following induction of long-term potentiation in the dentate gyrus of anaesthetized rats. Neurosci Lett. 1994;169:77–80

Feng J, et al. High frequency of neurexin 1β signal peptide structural variants in patients with autism. Neurosci Lett 2006;409:10–13

Flores, C.E., Nikonenko, I., Mendez, P., Fritschy, J.-M., Tyagarajan, S.K., and Muller, D. (2015). Activity-dependent inhibitory synapse remodeling through gephyrin phosphorylation. Proc. Natl. Acad. Sci. 112, E65–E72

Foldy, C., Malenka, R. C., and Sudhof, T. C. (2013). Autism-associated neuroligin- 3 mutations commonly disrupt tonic endocannabinoid signaling. Neuron 78, 498–509

Freund, T. F., Katona, I., and Piomelli, D. (2003). Role of endogenous cannabinoids in synaptic signaling. Physiol. Rev. 83, 1017–66

Gainey, M.A., and Feldman, D.E. (2017). Multiple shared mechanisms for homeostatic plasticity in rodent somatosensory and visual cortex. Philos. Trans. R. Soc. Lond. B Biol. Sci. 372, 372

Gatto, C. L., and Broadie, K. (2010). Genetic controls balancing excitatory and inhibitory synaptogenesis in neurodevelopmental disorder models. Front. Synaptic Neurosci. 2:4. doi: 10.3389/fnsyn.2010.00004

Genoux D, Montgomery JM. Glutamate receptor plasticity at excitatory synapses in the brain. Clin Exp Pharmacol Physiol. 2007 Oct;34(10):1058-63

Gerdeman, G.L., Ronesi, J., and Lovinger, D.M. (2002). Postsynaptic endocannabinoid release is critical to long-term depression in the striatum. Nat. Neurosci. 5, 446–451

Gibson, J.R., Bartley, A.F., Hays, S.A., and Huber, K.M. (2008). Imbalance of neocortical excitation and inhibition and altered UP states reflect network hyperexcitability in the mouse model of fragile X syndrome. J. Neurophysiol.100, 2615–2626

Gillberg C Coleman M . Autism and medical disorders: A review of the literature. Dev Med Child Neurol, 1996;38:191–202

Graf, E. R., Zhang, X., Jin, S.-X., Linhoff, M. W., & Craig, A. M. (2004). Neurexins induce differentiation of GABA and glutamate postsynaptic specializations via neuroligins. Cell, 119(7), 1013–26. doi:10.1016/j.cell.2004.11.035

Gray EG. 1959. Axo-somatic and axo-dendritic synapses of the cerebral cortex: An electron microscope study. J Anat 93: 420–433

Greger IH, Ziff EB, Penn AC (August 2007). "Molecular determinants of AMPA receptor subunit assembly". Trends in Neurosciences. 30 (8): 407–16

Guang, S., Pang, N., Deng, X., Yang, L., He, F., Wu, L., Chen, C., Yin, F., Peng, J., 2018. Synaptopathology involved in autism spectrum disorder. Front. Cell. Neurosci. 12, 470

Haklai-Topper L, Soutschek J, Sabanay H, Scheel J, Hobert O, Peles E. 2011. The neurexin superfamily of Caenorhabditis elegans. Gene Expr Patterns 11: 144–150

Hallmayer, J., Cleveland, S., Torres, A., Phillips, J., Cohen, B., Torigoe, T., et al. (2011). Genetic heritability and shared environmental factors among twin pairs with autism. Archives of General Psychiatry, 68(11), 1095–1102

Han, S., Tai, C., Westenbroek, R.E., Yu, F.H., Cheah, C.S., Potter, G.B., Rubenstein, J.L., Scheuer, T., de la Iglesia, H.O., and Catterall, W.A. (2012). Autistic-like behaviour in Scn1a+/- mice and rescue by enhanced GABA-mediated neurotransmission. Nature 489, 385–390

Happe´ F, Ronald A, Plomin R. Time to give up on a single explanation for autism. Nat Neurosci 2006;9(10):1218–20

Harkany, T., Holmgren, C., Hartig, W., Qureshi, T., Chaudhry, F. A., Storm-Mathisen, J., et al. (2004). Endocannabinoid-independent retrograde signaling at inhibitory synapses in layer 2/3 of neocortex: involvement of vesicular glutamate transporter 3. J. Neurosci. 24, 4978–4988

Harrington, A.J., Raissi, A., Rajkovich, K., Berto, S., Kumar, J., Molinaro, G., Raduazzo, J., Guo, Y., Loerwald, K., Konopka, G., et al. (2016). MEF2C regulates cortical inhibitory and excitatory synapses and behaviors relevant to neurodevelopmental disorders. eLife 5, 5

Hartman, K. N., Pal, S. K., Burrone, J. & Murthy, V. N. Activity-dependent regulation of inhibitory synaptic transmission in hippocampal neurons. Nat. Neurosci. 9, 642–649 (2006)

Hata Y, Butz S, Südhof TC. CASK: A novel dlg/PSD95 homologue with an N-terminal CaM kinase domain identified by interaction with neurexins. J Neurosci 1996;16:2488–2494

He, Q. et al. Interneuron- and GABAA receptor-specific inhibitory synaptic plasticity in cerebellar Purkinje cells. Nat. Commun. 6, 7364 (2015)

Heifets, B. D., and Castillo, P. E. (2009). Endocannabinoid signaling and long-term synaptic plasticity. Annu. Rev. Physiol. 71, 283–306

Heifets, B. D., Chevaleyre, V., and Castillo, P. E. (2008). Interneuron activity controls endocannabinoid-mediated presynaptic plasticity through calcineurin. Proc. Natl. Acad. Sci. U. S. A. 105, 10250–5

Hengen KB, Lambo ME, Van Hooser SD, Katz DB, Turrigiano GG. Firing rate homeostasis in visual cortex of freely behaving rodents. Neuron. 2013;80:335–42

Hoon, M., Soykan, T., Falkenburger, B., Hammer, M., Patrizi, A., Schmidt, K.-F., … Varoqueaux, F. (2011). Neuroligin-4 is localized to glycinergic postsynapses and regulates inhibition in the retina. Proceedings of the National Academy of Sciences of the United States of America, 108(7), 3053–8

Hosie, S.,Malone, D. T., Liu, S., Glass, M., Adlard, P. A., Hannan, A. J., et al. (2018). Altered Amygdala Excitation and CB1 Receptor Modulation of Aggressive Behavior in the Neuroligin-3(R451C) Mouse Model of Autism. Front. Cell Neurosci. 12:234

Houston, C. M., Lee, H. H., Hosie, A. M., Moss, S. J. & Smart, T. G. Identification of the sites for CaMK-IIdependent phosphorylation of GABAA receptors. J. Biol. Chem. 282, 17855–17865 (2007)

Howell BW, Smith KM. Synaptic structural protein dysfunction leads to altered excitation inhibition ratios in models of autism spectrum disorder. Pharmacol Res. 2019 Jan;139:207-214

Iascone DM, Li Y, Sümbül U, Doron M, Chen H, Andreu V, et al. Principles of excitatory and inhibitory synaptic organization constrain dendritic spiking in pyramidal neurons. BioRxiv. 2018 10.1101/395384

Ichtchenko K, et al. Neuroligin 1: A splice-site specific ligand for β-neurexins. Cell 1995;81:435–443

Ichtchenko K, Nguyen T, Südhof TC. Structures, alternative splicing, and neurexin binding of multiple neuroligins. J Biol Chem 1996;271:2676–2682

Iossifov I, Ronemus M, Levy D, Wang Z, Hakker I, Rosenbaum J, Yamrom B, Lee YH, Narzisi G, Leotta A, et al. (2012). De novo gene disruptions in children on the autistic spectrum. Neuron 74, 285–299

Iossifov, I., O'Roak, B. J., Sanders, S. J., Ronemus, M., Krumm, N., Levy, D., et al. (2014). The contribution of de novo coding mutations to autism spectrum disorder. Nature 515, 216–221

Irie, M., Hata, Y., Takeuchi, M., Ichtchenko, K., Toyoda, A., Hirao, K., … Südhof, T. C. (1997). Binding of neuroligins to PSD-95. Science (New York, N.Y.), 277(5331), 1511–5

Isshiki, M., Tanaka, S., Kuriu, T., Tabuchi, K., Takumi, T., and Okabe, S. (2014). Enhanced synapse remodelling as a common phenotype in mouse models of autism. Nat. Commun. 5:4742

Jamain S, Radyushkin K, Hammerschmidt K, Granon S, et al: Reduced social interaction and ultrasonic communication in a mouse model of monogenic heritable autism. Proc Natl Acad Sci USA 2008; 105: 1710–1715

Jamain, S., Quach, H., Betancur, C., Ra° stam, M., Colineaux, C., Gillberg, I.C., Soderstrom, H., Giros, B., Leboyer, M., Gillberg, C., et al. (2003). Mutations of the X-linked genes encoding neuroligins NLGN3 and NLGN4 are associated with autism. Nat. Genet. 34, 27–29

Jaramillo, T. C., Escamilla, C. O., Liu, S., Peca, L., Birnbaum, S. G., and Powell, C. M. (2018). Genetic background effects in Neuroligin-3 mutant mice: Minimal behavioral abnormalities on C57 background. Autism Res. 11, 234–244

Jaramillo, T. C., Liu, S., Pettersen, A., Birnbaum, S. G., and Powell, C. M. (2014). Autism-related neuroligin-3 mutation alters social behavior and spatial learning. Autism Res. 7, 264–272

Jiang, M., Polepalli, J., Chen, L. Y., Zhang, B., Sudhof, T. C., and Malenka, R. C. (2017). Conditional ablation of neuroligin-1 in CA1 pyramidal neurons blocks LTP by a cell-autonomous NMDA receptor-independent mechanism. Mol. Psychiatry 22, 375–383

Jiang, Y. H., Yuen, R. K., Jin, X., Wang, M., Chen, N., Wu, X., et al. (2013). Detection of clinically relevant genetic variants in autism spectrum disorder by whole-genome sequencing. Am. J. Hum. Genet. 93, 249–263

Kalbassi, S., Bachmann, S. O., Cross, E., Roberton, V. H., and Baudouin, S. J. (2017). Male and Female Mice Lacking Neuroligin-3 Modify the Behavior of Their Wild-Type Littermates. eNeuro 4:2017

Kano, M., Ohno-Shosaku, T., Hashimotodani, Y., Uchigashima, M., and Watanabe, M. (2009). Endocannabinoid-mediated control of synaptic transmission. Physiol. Rev. 89, 309–80

Kano, M., Rexhausen, U., Dreessen, J., and Konnerth, A. (1992). Synaptic excitation produces a long-lasting rebound potentiation of inhibitory synaptic signals in cerebellar Purkinje cells. Nature 356, 601–604

Kenny, E. M., Cormican, P., Furlong, S., Heron, E., Kenny, G., Fahey, C., et al. (2014). Excess of rare novel loss-of-function variants in synaptic genes in schizophrenia and autism spectrum disorders. Mol. Psychiatry 19, 872–879

Kim, E. Y., Schrader, N., Smolinsky, B., Bedet, C., Vannier, C., Schwarz, G., et al. (2006). Deciphering the structural framework of glycine receptor anchoring by gephyrin. EMBO J. 25, 1385–1395

Kirkwood, a, Dudek, S. M., Gold, J. T., Aizenman, C. D., and Bear, M. F. (1993). Common forms of synaptic plasticity in the hippocampus and neocortex in vitro. Science 260, 1518–1521. doi:10.1126/science.8502997

Kleijer KTE, et al. Neurobiology of autism gene products: towards pathogenesis and drug targets. Psychopharmacology. 2014;231(6):1037–62

Kneussel, M., and Betz, H. (2000b). Receptors, gephyrin and gephyrin-associated proteins: novel insights into the assembly of inhibitory postsynaptic membrane specializations. J. Physiol. 525 Pt 1, 1–9

Knott, G. W., Quairiaux, C., Genoud, C., & Welker, E. (2002). Formation of dendritic spines with GABAergic synapses induced by whisker stimulation in adult mice. Neuron, 34(2), 265–73

Ko, J., Zhang, C., Arac, D., Boucard, A. A., Brunger, A. T., and Sudhof, T. C. (2009). Neuroligin-1 performs neurexin-dependent and neurexin-independent functions in synapse validation. EMBO J. 28, 3244–3255

Kobayashi, K., Manabe, T., and Takahashi, T. (1996). Presynaptic Long-Term Depression at the Hippocampal Mossy Fiber--CA3 Synapse. Science (80-.). 273, 648–650

Kobayashi, K., Toshiya, M., and Tomoyuki, T. (1999). Calcium-dependent mechanisms involved in presynaptic long-term depression at the hippocampal mossy fibreCA3 synapse. Eur. J. Neurosci. 11, 1633–1638

Koehnke, J., Katsamba, P. S., Ahlsen, G., Bahna, F., Vendome, J., Honig, B., et al. (2010). Splice form dependence of beta-neurexin/neuroligin binding interactions. Neuron 67, 61–74

Kuhn, P. H., Colombo, A. V., Schusser, B., Dreymueller, D., Wetzel, S., Schepers, U., et al. (2016). Systematic substrate identification indicates a central role for the metalloprotease ADAM10 in axon targeting and synapse function

Kurotani, T., Yamada, K., Yoshimura, Y., Crair, M. C. & Komatsu, Y. State-dependent bidirectional modification of somatic inhibition in neocortical pyramidal cells. Neuron 57, 905–916 (2008)

Lai, E. S. K., Nakayama, H., Miyazaki, T., Nakazawa, T., Tabuchi, K., Hashimoto, K., et al. (2021). An Autism-Associated Neuroligin-3 Mutation Affects Developmental Synapse Elimination in the Cerebellum. Front. Neural Circuits 15:676891

Lautz JD, Brown EA, Williams VanSchoiack AA, Smith SEP. Synaptic activity induces input-specific rearrangements in a targeted synaptic protein interaction network. J Neurochem. 2018 Sep;146(5):540-559

Lawson-Yuen A, Saldivar JS, Sommer S, Picker J. Familial deletion within NLGN4 associated with autism and Tourette syndrome. Eur J Hum Genet 2008;16:614–618

Lee H-K, Kameyama K, Huganir RL, Bear MF. NMDA induces long-term synaptic depression and dephosphorylation of the GluR1 subunit of AMPA receptors in hippocampus. Neuron. 1998;21:1151–1162

Lee, H.-K., and Kirkwood, A. (2011). AMPA receptor regulation during synaptic plasticity in hippocampus and neocortex. Semin. Cell Dev. Biol. 22, 514–520

Levinson, J.N., El-Husseini, A., 2005. Building excitatory and inhibitory synapses: balancing neuroligin partnerships. Neuron 48, 171–174

Liang, J., Xu, W., Hsu, Y.T., Yee, A.X., Chen, L., and S€udhof, T.C. (2015). Conditional knockout of Nlgn2 in the adult medial prefrontal cortex (mPFC) induces delayed loss of inhibitory synapses. Mol. Psychiatry 20, 793

Lisman and Zhabotinsky, 2001 J.E. Lisman, A.M. Zhabotinsky. A model of synaptic memory: a CaMKII/PP1 switch that potentiates transmission by organizing an AMPA receptor anchoring assembly. Neuron, 31 (2001), pp. 191-201

Liu, J. J., Grace, K. P., Horner, R. L., Cortez, M. A., Shao, Y., and Jia, Z. (2017). Neuroligin 3 R451C mutation alters electroencephalography spectral activity in an animal model of autism spectrum disorders. Mol. Brain 10:10

Loke, Y. J., Hannan, A. J., and Craig, J. M. (2015). The role of epigenetic change in autism spectrum disorders. Front. Neurol. 6:107. doi: 10.3389/fneur.2015.00107

Loomes, R., Hull, L., & Mandy, W. P. L. (2017). What is the male-to-female ratio in autism spectrum disorder? A systematic review and meta-analysis. Journal of the American Academy of Child and Adolescent Psychiatry, 56(6), 466–474

Low, K., Crestani, F., Keist, R., Benke, D., Brunig, I., Benson, J. A., Fritschy, J. M., Rulicke, T., Bluethmann, H., Mohler, H., et al. (2000) Science 290, 131–134

Lu, Y. M., Mansuy, I. M., Kandel, E. R., and Roder, J. (2000). Calcineurinmediated LTD of GABAergic inhibition underlies the increased excitability of CA1 neurons associated with LTP. Neuron 26, 197–205

Lüthl A, Laurent JP, Figurov A, Muller D, Schachner M. Hippocampal long-term potentiation and neural cell adhesion molecules L1 and NCAM. Nature. 1994;372:777–779

Mahfouz, A., Ziats, M. N., Rennert, O. M., Lelieveldt, B. P., and Reinders, M. J. (2015). Shared pathways among autism candidate genes determined by co-expression network analysis of the developing human brain transcriptome. J. Mol. Neurosci. 57, 580–594. doi: 10.1007/s12031-015-0641-3

Malenka, R. C. & Bear, M. F. LTP and LTD: an embarrassment of riches. Neuron 44, 5–21n (2004)

Mao, W., Watanabe, T., Cho, S., Frost, J.L., Truong, T., Zhao, X., and Futai, K. (2015). Shank1 regulates excitatory synaptic transmission in mouse hippocampal parvalbumin-expressing inhibitory interneurons. Eur. J. Neurosci. 41, 1025–1035

Marder E, Goaillard J-M. Variability, compensation and homeostasis in neuron and network function. Nat Rev Neurosci. 2006; 7:563–574

Marsden, K.C., Beattie, J.B., Friedenthal, J., and Carroll, R.C. (2007). NMDA Receptor Activation Potentiates Inhibitory Transmission through GABA Receptor-Associated Protein-Dependent Exocytosis of GABAA Receptors. J. Neurosci. 27, 14326–14337

Marsden, K.C., Shemesh, A., Bayer, K.U., and Carroll, R.C. (2010). Selective translocation of Ca2+/calmodulin protein kinase II (CaMKII) to inhibitory synapses. Proc. Natl. Acad. Sci. 107, 20559–20564

Marshall CR. Structural variation of chromosomes in autism spectrum disorder. Am J Hum Genet 2008;82:477–488

Marsicano, G., Wotjak, C.T., Azad, S.C., Bisogno, T., Rammes, G., Cascio, M.G., Hermann, H., Tang, J., Hofmann, C., Zieglga¨ nsberger, W., et al. (2002). The endogenous cannabinoid system controls extinction of aversive memories. Nature 418, 530–534

Martella, G., Meringolo, M., Trobiani, L., De Jaco, A., Pisani, A., and Bonsi, P. (2018). The neurobiological bases of autism spectrum disorders: the R451Cneuroligin 3 mutation hampers the expression of long-term synaptic depression in the dorsal striatum. Eur. J. Neurosci. 47, 701–708

Matta, S. M., Moore, Z., Walker, F. R., Hill-Yardin, E. L., and Crack, P. J. (2020). An altered glial phenotype in the NL3(R451C) mouse model of autism. Sci. Rep. 10:14492

Medina, M. A., Andrade, V. M., Caracci, M. O., Avila, M. E., Verdugo, D. A., Vargas, M. F., et al. (2018). Wnt/beta-catenin signaling stimulates the expression and synaptic clustering of the autism-associated Neuroligin 3 gene. Transl. Psychiatry 8:45

Mellor, J., and Nicoll, R.A. (2001). Hippocampal mossy fiber LTP is independent of postsynaptic calcium. Nat. Neurosci. 4, 125–126

Merrill, M. A., Chen, Y., Strack, S., & Hell, J. W. (2005). Activity-driven postsynaptic translocation of CaMKII. Trends in Pharmacological Sciences, 26(12), 645–53

Missler M, et al. α-Neurexins couple Ca2+ channels to synaptic vesicle exocytosis. Nature 2003;423:939–948

Modi, B., Pimpinella, D., Pazienti, A., Zacchi, P., Cherubini, E., and Griguoli, M. (2019). Possible Implication of the CA2 Hippocampal Circuit in Social Cognition Deficits Observed in the Neuroligin 3 Knock-Out Mouse, a Non- Syndromic Animal Model of Autism. Front. Psychiatry 10:513

Monyer H, Burnashev N, Laurie DJ, Sakmann B, Seeburg PH. Developmental and regional expression in the rat brain and functional properties of four NMDA receptors. Neuron. 1994 Mar;12(3):529-40

Morris RG. Synaptic plasticity and learning: Selective impairment of learning rats and blockade of long-term potentiation in vivo by the N-methyl-d-aspartate receptor antagonist AP5. J. Neurosci. 1989; 9:3040–57

Moss, S. J., and Smart, T. G. (2001). Constructing inhibitory synapses. Nat. Rev. Neurosci. 2, 240–250

Muir, J., Arancibia-Carcamo, I.L., MacAskill, A.F., Smith, K.R., Griffin, L.D., and Kittler, J.T. (2010). NMDA receptors regulate GABAA receptor lateral mobility and clustering at inhibitory synapses through serine 327 on the 2 subunit. Proc. Natl. Acad. Sci. *107*, 16679–16684

Mulkey, R.M., Endo, S., Shenolikar, S., and Malenka, R.C. (1994a). Involvement of a calcineurin/inhibitor-1 phosphatase cascade in hippocampal long-term depression. Nature 369, 486–488

Nagy, V., Bozdagi, O., Matynia, A., Balcerzyk, M., Okulski, P., Dzwonek, J., … Huntley, G. W. (2006). Matrix metalloproteinase-9 is required for hippocampal late-phase long-term potentiation and memory. The Journal of Neuroscience : The Official Journal of the Society for Neuroscience, 26(7), 1923–34

Nakanishi, M., Nomura, J., Ji, X., Tamada, K., Arai, T., Takahashi, E., Bucan, M., and Takumi, T. (2017). Functional significance of rare neuroligin 1 variants found in autism. PLoS Genet. 13, e1006940

Nam CI, Chen L. Postsynaptic assembly induced by neurexin-neuroligin interaction and neurotransmitter. Proc Natl Acad Sci USA 2005;102:6137–6142

Neale BM, Kou Y, Liu L, et al.: Patterns and rates of exonic de novo mutations in autism spectrum disorders. Nature 2012; 485:242–245

Nelson, S. B., and Valakh, V. (2015). Excitatory/inhibitory balance and circuit homeostasis in autism spectrum disorders. Neuron 87, 684–698

Nicoll, R. a, and Schmitz, D. (2005). Synaptic plasticity at hippocampal mossy fibre synapses. Nat. Rev. Neurosci. 6, 863–76. doi:10.1038/nrn1786

Niedringhaus M, Chen X, Dzakpasu R, Conant K. MMPs and soluble ICAM-5 increase neuronal excitability within in vitro networks of hippocampal neurons. PLOS ONE. 2012;7(8):1–9

Niwa, F. et al. Gephyrin-independent GABAAR mobility and clustering during plasticity. PLOS ONE 7, e36148 (2012)

Norris, R. H. C., Churilov, L., Hannan, A. J., and Nithianantharajah, J. (2019). Mutations in neuroligin-3 in male mice impact behavioral flexibility but not relational memory in a touchscreen test of visual transitive inference. Mol. Autism 10:42

Nusser, Z., Hájos, N., Somogyi, P., and Mody, I. (1998). Increased number of synaptic GABAA receptors underlies potentiation at hippocampal inhibitory synapses. Nature 395, 172–177

Ohno-Shosaku, T., Maejima, T., and Kano, M. (2001). Endogenous cannabinoids mediate retrograde signals from depolarized postsynaptic neurons to presynaptic terminals. Neuron 29, 729–738

Oliveira B, et al. Excitation-inhibition dysbalance as predictor of autistic phenotypes. J Psychiatr Res. 2018;104:96–9

O'Roak BJ, et al. Multiplex targeted sequencing identifies recurrently mutated genes in autism spectrum disorders. Science. 2012;338 (6114):1619-1622

Ozonoff, S., Young, G. S., Carter, A., Messinger, D., Yirmiya, N., Zwaigenbaum, L., et al. (2011). Recurrence risk for autism spectrum disorders: A baby siblings research consortium study. Pediatrics, 128(3), 488–495

Palade GE, Palay SL. 1954. Electron microscope observations of interneuronal and neuromuscular synapses. Anat Record 118: 335–336

Palmer, N., Beam, A., Agniel, D., Eran, A., Manrai, A., Spettell, C., et al. (2017). Association of sex with recurrence of autism spectrum disorder among siblings. JAMA Pediatrics, 171(11), 1107–1112

Peixoto, R. T., Kunz, P. A., Kwon, H., Mabb, A. M., Sabatini, B. L., Philpot, B. D., & Ehlers, M. D. (2012). Transsynaptic Signaling by Activity-Dependent Cleavage of Neuroligin-1. Neuron, 76(2), 396–409

Peng, Y. R. et al. Postsynaptic spiking homeostatically induces cell-autonomous regulation of inhibitory inputs via retrograde signaling. J. Neurosci. 30, 16220–16231 (2010)

Pennacchietti F, Vascon S, Nieus T, Rosillo C, Das S, Tyagarajan SK, Diaspro A, Del Bue A, Petrini EM, Barberis A, Cella Zanacchi F. Nanoscale Molecular Reorganization of the Inhibitory Postsynaptic Density Is a Determinant of GABAergic Synaptic Potentiation. J Neurosci. 2017 Feb 15;37(7):1747-1756

Persico, A. M., & Sacco, R. (2014). Endophenotypes in autism spectrum disorders. In Comprehensive guide to autism (pp. 77–95). New York: Springer

Petrini, E. M., Nieus, T., Ravasenga, T., Succol, F., Guazzi, S., Benfenati, F., & Barberis, A. (2011). Influence of GABAAR monoliganded states on GABAergic responses. The Journal of Neuroscience : The Official Journal of the Society for Neuroscience, 31(5), 1752–61

Petrini, E.M., and Barberis, A. (2014). Diffusion dynamics of synaptic molecules during inhibitory postsynaptic plasticity. Front. Cell. Neurosci. 8, 1–16

Philibert, R. A., Winfield, S. L., Sandhu, H. K., Martin, B. M., and Ginns, E. I. (2000). The structure and expression of the human neuroligin-3 gene. Gene 246, 303–310

Piechotta, K., Dudanova, I., & Missler, M. (2006). The resilient synapse: insights from genetic interference of synaptic cell adhesion molecules. Cell and Tissue Research, 326(2), 617–42. doi:10.1007/s00441-006-0267-4

Polepalli, J. S., Wu, H., Goswami, D., Halpern, C. H., Sudhof, T. C., and Malenka, R. C. (2017). Modulation of excitation on parvalbumin interneurons by neuroligin-3 regulates the hippocampal network. Nat. Neurosci. 20, 219–229

Polsky A, Mel BW, Schiller J. Computational subunits in thin dendrites of pyramidal cells. Nat Neurosci. 2004 Jun;7(6):621-7

Poulopoulos, A., Aramuni, G., Meyer, G., Soykan, T., Hoon, M., Papadopoulos, T., … Varoqueaux, F. (2009). Neuroligin 2 drives postsynaptic assembly at perisomatic inhibitory synapses through gephyrin and collybistin. Neuron, 63(5), 628–42

Poulopoulos, A., Soykan, T., Tuffy, L. P., Hammer, M., Varoqueaux, F., and Brose, N. (2012). Homodimerization and isoform-specific heterodimerization of neuroligins. Biochem. J. 446, 321–330

Pozo K, Goda Y. Unraveling mechanisms of homeostatic synaptic plasticity. Neuron. 2010; 66:337–351

Proctor, D. T., Stotz, S. C., Scott, L. O. M., de la Hoz, C. L. R., Poon, K. W. C., Stys, P. K., et al. (2015). Axo-glial communication through neurexin-neuroligin signaling regulates myelination and oligodendrocyte differentiation. Glia 63, 2023–2039

Quartier, A., Courraud, J., Thi, Ha, T., McGillivray, G., Isidor, B., et al. (2019). Novel mutations in NLGN3 causing autism spectrum disorder and cognitive impairment. Hum. Mutat. 40, 2021–2032

Radyushkin, K., Hammerschmidt, K., Boretius, S., Varoqueaux, F., El-Kordi, A., Ronnenberg, A., … Ehrenreich, H. (2009). Neuroligin-3-deficient mice: model of a monogenic heritable form of autism with an olfactory deficit. Genes, Brain, and Behavior, 8(4), 416–25. doi:10.1111/j.1601-183X.2009.0048

Redin, C., Gerard, B., Lauer, J., Herenger, Y., Muller, J., Quartier, A., et al. (2014). Efficient strategy for the molecular diagnosis of intellectual disability using targeted high-throughput sequencing. J. Med. Genet. 51, 724–736

Rees, R. P., Bunge, M. B., & Bunge, R. P. (1976). Morphological changes in the neuritic growth cone and target neuron during synaptic junction development in culture. The Journal of Cell Biology, 68(2), 240–63

Regehr, W. G., Carey, M. R., and Best, A. R. (2009). Activity-Dependent Regulation of Synapses by Retrograde Messengers. Neuron 63, 154–170

Reiss K, Maretzky T, Ludwig A, Tousseyn T, de Strooper B, Hartmann D, Saftig P. ADAM10 cleavage of N-cadherin and regulation of cell-cell adhesion and beta-catenin nuclear signalling. EMBO J. 2005;24(4):742–752

Renner, M., Choquet, D., & Triller, A. (2009). Control of the postsynaptic membrane viscosity. The Journal of Neuroscience : The Official Journal of the Society for Neuroscience, 29(9), 2926–37

Robbe, D., Kopf, M., Remaury, A., Bockaert, J., and Manzoni, O.J. (2002). Endogenous cannabinoids mediate long-term synaptic depression in the nucleus accumbens. Proc. Natl. Acad. Sci. USA 99, 8384–8388

Rothwell, P. E., Fuccillo, M. V., Maxeiner, S., Hayton, S. J., Gokce, O., Lim, B. K., et al. (2014). Autism-associated neuroligin-3 mutations commonly impair striatal circuits to boost repetitive behaviors. Cell 158, 198–212

Rubenstein JL, Merzenich MM. Model of autism: increased ratio of excitation/inhibition in key neural systems. Genes Brain Behav. 2003 Oct;2(5):255-67. doi: 10.1034/j.1601-183x.2003.00037.x.

Rutter M. Diagnosis and defi nition of childhood autism. J Autism Child Schizophr 1978; 8: 139–61

Salussolia CL, Prodromou ML, Borker P, Wollmuth LP (August 2011). "Arrangement of subunits in functional NMDA receptors". The Journal of Neuroscience. 31 (31): 11295–11304

Sanders SJ, Murtha MT, Gupta AR, et al.: De novo mutations revealed by whole-exome sequencing are strongly associated with autism. Nature 2012; 485:237–241

Sandin, S., Lichtenstein, P., Kuja-Halkola, R., Hultman, C., Larsson, H., Reichenberg, A. (2017). The heritability of autism spectrum disorder. JAMA, 318, 1182. https://doi.org/10.1001/jama.2017.12141

Scheiffele, P., Fan, J., Choih, J., Fetter, R., & Serafini, T. (2000). Neuroligin expressed in nonneuronal cells triggers presynaptic development in contacting axons. Cell, 101(6), 657–69

Selten, M., van Bokhoven, H., and Nadif Kasri, N. (2018). Inhibitory control of the excitatory/inhibitory balance in psychiatric disorders. F1000Res. 7, 23

Shen, K., & Meyer, T. (1999). Dynamic control of CaMKII translocation and localization in hippocampal neurons by NMDA receptor stimulation. Science (New York, N.Y.), 284(5411), 162–6

Shipman, S. L., and Nicoll, R. A. (2012b). Dimerization of postsynaptic neuroligin drives synaptic assembly via transsynaptic clustering of neurexin. Proc. Natl. Acad. Sci. U S A. 109, 19432–19437

Sieghart, W. (2006). Structure, Pharmacology, and Function of GABAA Receptor Subtypes. Adv. Pharmacol. 54, 231–263. doi:10.1016/S1054-3589(06)54010-4

Sieghart, W., and Sperk, G. (2002). Subunit composition, distribution and function of GABA(A) receptor subtypes. Curr. Top. Med. Chem. 2, 795–816

Sjöström PJ, Nelson SB. Spike timing, calcium signals and synaptic plasticity. Curr Opin Neurobiol. 2002 Jun;12(3):305-14

Smith, K. R., Jones, K. A., Kopeikina, K. J., Burette, A. C., Copits, B. A., Yoon, S., Forrest, M. P., Fawcett-Patel, J. M., Hanley, J. G., Weinberg, R. J., Swanson, G. T., & Penzes, P. (2017). Cadherin-10 maintains excitatory/inhibitory ratio through interactions with synaptic proteins. Journal of Neuroscience, 37(46), 11127-11139

Sobczyk A, Scheuss V, Svoboda K. NMDA receptor subunit-dependent [Ca2+] signaling in individual hippocampal dendritic spines. J Neurosci. 2005 Jun 29;25(26):6037-46

Sola, M., Bavro, V. N., Timmins, J., Franz, T., Ricard-Blum, S., Schoehn, G., et al. (2004). Structural basis of dynamic glycine receptor clustering by gephyrin. EMBO J. 23, 2510–9

Sommer B, Monyer H, Wisden W et al. Glutamate-gated ion channels in the brain. Genetic mechanism for generating molecular and functional diversity. Arzneimittelforschung 1992; 42: 209–10

Speed, H. E.,Masiulis, I., Gibson, J. R., and Powell, C. M. (2015). Increased Cortical Inhibition in Autism-Linked Neuroligin-3R451C Mice Is Due in Part to Loss of Endocannabinoid Signaling. PLoS One 10:e0140638

Stogsdill, J. A., Ramirez, J., Liu, D., Kim, Y. H., Baldwin, K. T., Enustun, E., et al. (2017). Astrocytic neuroligins control astrocyte morphogenesis and synaptogenesis. Nature 551, 192–197

Subramanian, M., Timmerman, C. K., Schwartz, J. L., Pham, D. L., and Meffert, M. K. (2015). Characterizing autism spectrum disorders by key biochemical pathways. Front. Neurosci. 9:313. doi: 10.3389/fnins.2015.00313

Südhof, T. C. (2008). Neuroligins and neurexins link synaptic function to cognitive disease. Nature, 455(7215), 903–911. doi:10.1038/nature07456

Tabuchi K, Südhof TC. Structure and evolution of neurexin genes: insight into the mechanism of alternative splicing. Genomics 2002;79:849–859

Tabuchi, K., Blundell, J., Etherton, M.R., Hammer, R.E., Liu, X., Powell, C.M., and Sudhof, T.C. (2007). A neuroligin-3 mutation implicated in autism increases inhibitory synaptic transmission in mice. Science 318, 71–76

Toni, N., Buchs, P. A., Nikonenko, I., Bron, C. R., & Muller, D. (1999). LTP promotes formation of multiple spine synapses between a single axon terminal and a dendrite. Nature, 402(6760), 421–5. doi:10.1038/46574

Trobiani, L., Favaloro, F. L., Di Castro, M. A., Di Mattia, M., Cariello, M., Miranda, E., et al. (2018). UPR activation specifically modulates glutamate neurotransmission in the cerebellum of a mouse model of autism. Neurobiol. Dis. 120, 139–150

Turrigiano GG, Nelson SB. Homeostatic plasticity in the developing nervous system. Nat Rev Neurosci. 2004; 5:97–107

Turrigiano, G. (2011). Too many cooks? Intrinsic and synaptic homeostatic mechanisms in cortical circuit refinement. Annu. Rev. Neurosci. 34, 89–103

Tzounopoulos, T., Janz, R., Südhof, T.C., Nicoll, R.A., and Malenka, R.C. (1998). A role for cAMP in long-term depression at hippocampal mossy fiber synapses. Neuron 21, 837–845

Uchigashima M, Cheung A and Futai K (2021) Neuroligin-3: A Circuit-Specific Synapse Organizer That Shapes Normal Function and Autism Spectrum Disorder-Associated Dysfunction. Front. Mol. Neurosci. 14:749164

Uchigashima, M., Leung, M., Watanabe, T., Cheung, A., Le, T., Pallat, S., et al. (2020b). Neuroligin3 splice isoforms shape inhibitory synaptic function in the mouse hippocampus. J. Biol. Chem. 295, 8589–8595

Ullrich B, Ushkaryov YA, Südhof TC. Cartography of neurexins: More than 1000 isoforms generated by alternatice splicing and expressed in distinct subsets of neurons. Neuron 1995;14:497–507

Unichenko, P., Yang, J.W., Kirischuk, S., Kolbaev, S., Kilb, W., Hammer, M., Krueger-Burg, D., Brose, N., and Luhmann, H.J. (2018). Autism related Neuroligin-4 knockout impairs intracortical processing but not sensory inputs in mouse barrel cortex. Cereb. Cortex 28, 2873–2886

Unwin, N. (1995). Acetylcholine receptor channel imaged in the open state. Nature, 373(6509), 37–43. doi:10.1038/373037a0

Ushkaryov YA, Petrenko AG, Geppert M, Südhof TC. Neurexins: Synaptic cell surface proteins related to the α-latrotoxin receptor and laminin. Science 1992;257:40–56.Reports the discovery of Nrxns as presynaptic α-latrotoxin receptors

Ushkaryov YA, Rohou A, Sugita S. α-Latrotoxin and its receptors. Handb Exp Pharmacol 2008;184:171–206

Ushkaryov, Y. A., Hata, Y., Ichtchenko, K., Moomaw, C., Afendis, S., Slaughter, C. A., & Südhof T. C. (1994). Conserved domain structure of beta-neurexins. Unusual cleaved signal sequences in receptor-like neuronal cell-surface proteins. The Journal of Biological Chemistry, 269(16), 11987–92

Varoqueaux F, Aramuni G, Rawson RL,Mohrmann R, Missler M, Gottmann K, ZhangW, Su¨dhof TC, Brose N. 2006. Neuroligins determine synapse maturation and function. Neuron 51: 741–754

Varoqueaux F, Jamain S, Brose N. Neuroligin 2 is exclusively localized to inhibitory synapses. Eur J Cell Biol 2004;83:449–456

Venkatesh, H. S., Tam, L. T., Woo, P. J., Lennon, J., Nagaraja, S., Gillespie, S. M., et al. (2017). Targeting neuronal activity-regulated neuroligin-3 dependency in high-grade glioma. Nature 549, 533–537

Wang, X., Bozdagi, O., Nikitczuk, J. S., Zhai, Z. W., Zhou, Q., & Huntley, G. W. (2008). Extracellular proteolysis by matrix metalloproteinase-9 drives dendritic spine enlargement and long-term potentiation coordinately. Proceedings of the National Academy of Sciences of the United States of America, 105(49), 19520–5

Wen, Y., Alshikho, M. J., and Herbert, M. R. (2016). Pathway network analyses for autism reveal multisystem involvement, major overlaps with other diseases and convergence upon MAPK and calcium signaling. PLoS ONE 11:e0153329. doi: 10.1371/journal.pone.0153329

Whiting, P. J. (2003). GABA-A receptor subtypes in the brain: a paradigm for CNS drug discovery? Drug Discov. Today 8, 445–450

Wiera, G., Lebida, K., Lech, A.M. et al. Long-term plasticity of inhibitory synapses in the hippocampus and spatial learning depends on matrix metalloproteinase 3. Cell. Mol. Life Sci. 78, 2279–2298 (2021)

Wiera, G., Lebida, K., Lech, A.M. et al. Long-term plasticity of inhibitory synapses in the hippocampus and spatial learning depends on matrix metalloproteinase 3. Cell. Mol. Life Sci. 78, 2279–2298 (2021)

Wilson, R.I., and Nicoll, R.A. (2001). Endogenous cannabinoids mediate retrograde signalling at hippocampal synapses. Nature 410, 588–592

Wood, L., and Shepherd, G.M.G. (2010). Synaptic circuit abnormalities of motor-frontal layer 2/3 pyramidal neurons in a mutant mouse model of Rett syndrome. Neurobiol. Dis. 38, 281–287

Xu, X., Xiong, Z., Zhang, L., Liu, Y., Lu, L., Peng, Y., et al. (2014). Variations analysis of NLGN3 and NLGN4X gene in Chinese autism patients. Mol. Biol. Rep. 41, 4133–4140

Yong, V. W. (2005). Metalloproteinases: mediators of pathology and regeneration in the CNS. Nature Reviews. Neuroscience, 6(12), 931–44

Yoshida, T., Yamagata, A., Imai, A., Kim, J., Izumi, H., Nakashima, S., et al. (2021). Canonical versus non-canonical transsynaptic signaling of neuroligin 3 tunes development of sociality in mice. Nat. Commun. 12:1848

Yu, T. W., Chahrour, M. H., Coulter, M. E., Jiralerspong, S., Okamura-Ikeda, K., Ataman, B., et al. (2013). Using whole-exome sequencing to identify inherited causes of autism. Neuron 77, 259–273

Yuen, R. K. C., Thiruvahindrapuram, B., Merico, D., Walker, S., Tammimies, K., Hoang, N., et al. (2015). Whole-genome sequencing of quartet families with autism spectrum disorder. Nature Medicine, 21(2), 185–191

Yuen, R.K. C., Merico, D., Bookman, M., Jennifer, L. H., Thiruvahindrapuram, B., Patel, R. V., et al. (2017). Whole genome sequencing resource identifies 18 new candidate genes for autism spectrum disorder. Nat. Neurosci. 20, 602–611

Zalutsky, R.A., and Nicoll, R.A. (1990). Comparison of two forms of long-term potentiation in single hippocampal neurons. Science (80-.). 248, 1619–1624

Zeidan J, Fombonne E, Scorah J, Ibrahim A, Durkin MS, Saxena S, Yusuf A, Shih A, Elsabbagh M. Global prevalence of autism: A systematic review update. Autism Res. 2022 May;15(5):778-790

Zhang W, et al. Extracellular domains of α-neurexins participate in regulating synaptic transmission by selectively affecting N-and P/Q-type Ca2+ -channels. J Neurosci 2005;25:4330–4342

Zhang, B., Chen, L.Y., Liu, X., Maxeiner, S., Lee, S.-J., Gokce, O., Südhof, T.C., 2015. Neuroligins sculpt cerebellar purkinje-cell circuits by differential control of distinct classes of synapses. Neuron 87, 781–796

Zhang, Y., Chen, K., Sloan, S. A., Bennett, M. L., Scholze, A. R., O'Keeffe, S., et al. (2014). An RNA-sequencing transcriptome and splicing database of glia, neurons, and vascular cells of the cerebral cortex. J. Neurosci. 34, 11929–11947

Zhang, Y.-P., Holbro, N., & Oertner, T. G. (2008). Optical induction of plasticity at single synapses reveals input-specific accumulation of alphaCaMKII. Proceedings of the National Academy of Sciences of the United States of America, 105(33), 12039–44. doi:10.1073/pnas.0802940105

Zoghbi HY, Bear MF. Synaptic dysfunction in neurodevelopmental disorders associated with autism and intellectual disabilities. Cold Spring Harb. Perspect. Biol. 2012;4(3)

ACKNOWLEDGEMENTS

First and foremost I would like to express my deepest gratitude to my supervisors, *Andrea* and *Enrica*. Their immense knowledge and plentiful experience have encouraged me in all the time of my academic research and daily life.

I would also like to thank all my current and former colleagues. They are not just my lab mates but also my "big family" in Genoa. Each of them has taught me something and I would not have gotten this far without them. Thanks to *Tiziana*, *Alice*, *Max, Stefania, Bea, Vincenzo, Dario, Amber*, *Sara*, *Mattia, Martina*, *Niccolò* and *Maithe*.

I am also thankful to my best friends, *Marta* and *Giulia*, even if physically distant, they always believed in me and made me feel their support.

Words cannot express my gratitude to my *Mum* and *Dad*, they made this happen and I will always be grateful for what they have sacrificed to make my dreams come true.

Many thanks to my sister, *Altea* and my brothers, *Davide* and *Alessandro*; they are simply the most valuable thing I have in this world.

A special thanks to my *Grandma Anna,* her love has guided me at every step of my life.

Finally yet importantly, I am extremely grateful to *Francesco*, my future husband. He, more than anyone, has always been there for me during this challenging journey. He gave me the strength to become who I am today. Thanks for the patience, the support and the tireless love.